



Diel variations in cell division and biomass production of *Emiliana huxleyi*—Consequences for the calculation of physiological cell parameters

Dorothee M. Kottmeier ^{1,2*} Anja Terbrüggen,² Dieter A. Wolf-Gladrow,² Silke Thoms²

¹The Marine Biological Association, Plymouth, United Kingdom

²Alfred Wegener Institute, Helmholtz Centre for Polar and Marine Research, Bremerhaven, Germany

Abstract:

Cell division of the coccolithophore *Emiliana huxleyi* and other phytoplankton typically becomes entrained to diel light/dark cycles under laboratory conditions, with division occurring primarily during dark phases and production occurring during light phases. Under these conditions, increases in cell and biomass concentrations deviate from exponential functions on time scales < 24 h. These deviations lead to significant diel variations in common measurements of phytoplankton physiology such as cellular quotas of particulate organic and inorganic carbon (POC, PIC) and their production rates. Being time-dependent, only the temporal mean of the various values during the day are comparable between experiments. Deviations from exponential growth furthermore imply that increases in cell and biomass concentrations cannot be expressed by the daily growth rate $\mu_{24\text{ h}}$ (typically determined from daily increments in cell concentrations). Consequently, conventional calculations of production as the product of a cellular quota (e.g., POC quota) and $\mu_{24\text{ h}}$ are mathematically incorrect. To account for this, we here describe short-term changes in cell and biomass concentrations of fast-dividing, dilute-batch cultures of *E. huxleyi* grown under a diel light/dark cycle using linear regression. Based on the derived models, we present calculations for daily means of cellular quotas and production rates. Conventional (time-specific) measurements of cellular quotas and production differ from daily means by up to 65% in our example and, under some circumstances, cause false “effects” of treatments. Intending to reduce errors in ecophysiological studies, we recommend determining daily means—mathematically or by adjusting the experimental setup or sampling times appropriately.

In ecophysiological laboratory studies on phytoplankton, “growth rates” are common measures for the physiological state of cultures under given environmental conditions. “Growth” of phytoplankton consists of an increase in biomass followed by cell division and production of two smaller daughter cells. This results in an exponential increase in biomass and cell concentration, when measurements are taken every 24 h. For the cell concentration N , the relationship between N and time (t) can be expressed as:

$$N(t) = N_{t_{0h}} \cdot e^{\mu_{24\text{ h}} \cdot t} \quad (1)$$

where $N_{t_{0h}}$ is the initial cell concentration (cells volume⁻¹) and $\mu_{24\text{ h}}$ (time⁻¹) is the “specific growth rate”, that is, strictly speaking, a rate constant (Guillard 1973; MacIntyre and Cullen 2005). During exponential growth, the rate of increase in the cell concentration is proportional to the concentration present:

$$\frac{dN}{dt} = N(t) \cdot \mu_{24\text{ h}} \quad (2)$$

In phytoplankton cultures that grow under diel light/dark cycles, cell division of most phytoplankton becomes *phased*, that is, cell division occurs in restricted periods of the day only (e.g., Nelson and Brand 1979; Harding et al. 1981). In the coccolithophore *Emiliana huxleyi*, cell division occurs primarily during dark phases, whereas biomass production naturally occurs only during light phases (Nelson and Brand 1979; Linschooten et al. 1991; Jochem and Meyerdierks 1999; Müller et al. 2008). In many phytoplankton cultures with phased division, cells fully or partially synchronize their cell

*Correspondence: dorkot@mba.ac.uk

This is an open access article under the terms of the Creative Commons Attribution License, which permits use, distribution and reproduction in any medium, provided the original work is properly cited.

Additional Supporting Information may be found in the online version of this article.

cycle, that is, cultures undergo the cell cycle simultaneously (Fig. 1; Hoogenhout 1963; Prison and Lorenzen 1966; Nelson and Brand 1979; Chisholm et al. 1984). When cell division (or biomass production) is phased, the increase in cell concentrations and biomass deviates from exponential functions on time scales < 24 h.

E. huxleyi is a widespread bloom-forming coccolithophore that, due to its ability to calcify, has long been in the focus of ecophysiological studies (Paasche 2001; Rost and Riebesell 2004; Zondervan 2007). Many ecophysiological studies estimate how environmental changes affect cell physiology by determining pool sizes of cellular components (e.g., cellular quotas of particulate organic carbon [POC] or particulate inorganic carbon [PIC] as measures for cellular biomass or calcite, respectively). Large pool sizes of a cell component do not necessarily imply large production rates of this component, but can also be a consequence of low division rates. Therefore, cellular production rates are often calculated from cellular pool sizes taking into account the specific growth rate $\mu_{24\text{ h}}$. Cellular POC or PIC production rates, for example, are commonly used as measures for photosynthetic carbon production or calcification, respectively (Raven and Crawford 2012; Meyer and Riebesell 2015). Such physiological cell parameters are commonly estimated from single measurements during the day, applying equations derived from exponential growth (for details, refer to the “Discussion” section). However, in cultures that are entrained to diel light/dark cycles, these equations do not apply and can introduce errors that can lead to misleading conclusions.

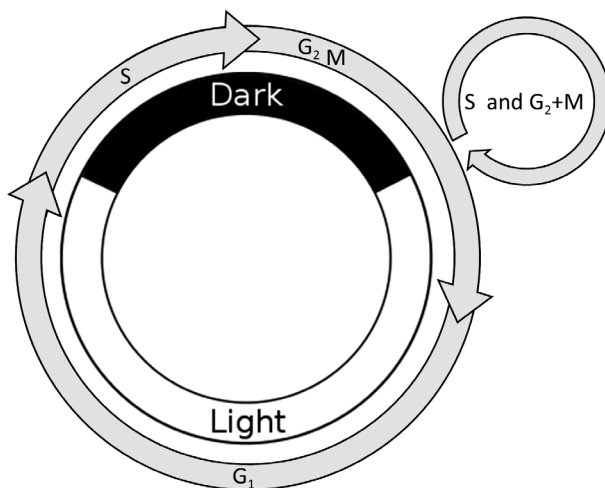


Fig. 1. Scheme of a phytoplankton cell cycle (modified after Howard and Pelc 1953). Four cell cycle phases are distinguished: In the G₁ phase, cells synthesize biomass such as carbohydrates and proteins. In the S phase, cells replicate their nuclear DNA. In the G₂ phase, cells prepare for mitosis. In the M phase, cell undergo mitosis and cytokinesis. Based on the findings of this study, we suggest that *E. huxleyi* may undergo two consecutive DNA replication/division phases (i.e., two subsequent S and G₂+M periods) when dividing more than once within 24 h.

The aim of this study is to deliver a detailed mathematical description of short-term growth kinetics of *E. huxleyi* cultures grown under light/dark cycles that allows for appropriate calculation of physiological cell parameters. For this purpose, we grew *E. huxleyi* as dilute batch cultures under a diel 16:8 h light/dark cycle and sampled cell, POC, and PIC concentrations (and some additional cell parameters) over a complete dark/light sequence in one hour intervals. Using linear regression, we derive stepwise linear functions quantitatively describing cell, POC, and PIC concentrations over the course of 24 h (“Phased division and production in *E. huxleyi*” section). We discuss how the phased division and production, and the resulting diel variations in cell and biomass concentrations, have consequences for the interpretation and determination of cellular pool sizes and production rates (“Diel variations in division and production require alternative estimates of ecophysiological responses” section). The stepwise linear functions describing the increase in cell as well as POC and PIC concentrations vs. time are then used to calculate daily means of cellular POC and PIC quotas, and cellular POC and PIC production rates. These daily means deliver parameters that are comparable between experiments and can be modified for different phytoplankton species (“Implications for the interpretation of existing research” section). We present that daily means can be either calculated applying the provided analytical equations, or by adjusting the experimental setup or sampling times accordingly.

Materials:

We monitored concentrations of cells, POC, and PIC as well as ratios of PIC : POC, POC : particulate organic nitrogen (PON), POC : cell volume, and chlorophyll *a* (Chl *a*) : POC of five *E. huxleyi* cultures (strain RCC 1216) that were acclimated to 16: 8 h light/dark cycles. The five cultures were grown under time-displaced light/dark cycles, that is, in the different cultures, the light/dark cycle was staggered to start at different local times (Table 1). This sampling regime allowed us to sample the full 24 h period within an 11 h sampling window. Each time point within the light/dark cycle was sampled in duplicates to triplicates (Table 1). Within the sampling period, data points were sampled in intervals of 1 h. For the analysis of the data, the beginning of the 8 h dark phase was defined as *initial* sampling time ($t = 0$ h). Because no samples were taken at the exact time point $t = 0$ h, all initial data were approximated by the data taken at $t = 0.5$ h.

Cells were cultured as dilute batch cultures in temperature-controlled culture rooms at 15°C, keeping cell concentrations at $< 70,000$ cells mL⁻¹ to avoid large drifts in nutrients and carbonate chemistry. Culturing was performed in polycarbonate bottles that were placed on roller tables. Bottles contained sterile-filtered (0.2 μm) North Sea water (salinity of 34). Seawater was enriched with metals and vitamins according to F/2_R medium (Guillard and Ryther 1962), with nitrate and

Table 1. Sampling regime.:

		Sampling period: 8.30h – 19.30h local time											
Times within dark/light cycle:													
<i>Culture I</i>	16.5 h	18.5 h	20.5 h	22.5 h	0.5 h	2.5 h	4.5 h	6.5 h	8.5 h	10.5 h	12.5 h	14.5 h	
<i>Culture II</i>	16.5 h	18.5 h	20.5 h	22.5 h	0.5 h	2.5 h	4.5 h	6.5 h	8.5 h	10.5 h	12.5 h	14.5 h	
<i>Culture III</i>	4.5 h	6.5 h	8.5 h	10.5 h	12.5 h	14.5 h	16.5 h	18.5 h	20.5 h	22.5 h	0.5 h	2.5 h	
<i>Culture IV</i>	10.5 h	12.5 h	14.5 h	16.5 h	18.5 h	20.5 h	22.5 h	0.5 h	2.5 h	4.5 h	6.5 h	8.5 h	
<i>Culture V</i>	22.5 h	0.5 h	2.5 h	4.5 h	6.5 h	8.5 h	10.5 h	12.5 h	14.5 h	16.5 h	18.5 h	20.5 h	
Local time	0 h	2 h	4 h	6 h	8 h	10 h	12 h	14 h	16 h	18 h	20 h	22 h	

Dark phase
 Light phase

The experiment was designed in order to ensure that two to three out of the five cultures were at the “correct” phase during the 11 h sampling period. Samples for time point $t = 0.5$ h (within the dark/light cycle; red numbers) were, for example, taken in triplicates (at 08.30 h local time in *Culture I* and *II*, and at 14.30 h local time in *Culture IV*). Samples for time point $t = 8.5$ h (within the dark/light cycle; blue numbers) were also taken in triplicates (at 16.30 h local time in *Culture I* and *II*, and at 10.30 h local time in *Culture V*). Samples for time point $t = 16.5$ h (within the dark/light cycle; green numbers) were taken as duplicates (at 12.30 h local time in *Culture III*, and at 18.30 h local time in *Culture V*).

phosphate concentrations of $110 \mu\text{mol L}^{-1}$ and $3 \mu\text{mol L}^{-1}$, respectively. Light was provided by Econlux SolarStinger Sunstrip LED lamps at an intensity of $195 \mu\text{mol photons m}^{-2} \text{s}^{-1}$. Cells were acclimated to the given conditions for at least 8 d prior to the beginning of the sampling period.

Cell concentrations and cell volumes were measured using a Coulter Counter (Multisizer 3, Beckman Coulter, Krefeld, Germany). Because absolute cell concentrations differed between the cultures, cell concentrations were normalized to the initial concentration of the respective culture. The resulting relative cell concentrations (N_{rel} , dimensionless) are defined as:

$$N_{\text{rel}} = N_t / N_{t_{0\text{h}}} \quad (3)$$

where N_t represents the measured time-specific cell concentrations of the different cultures (cells mL^{-1}) and $N_{t_{0\text{h}}}$ represents the respective initial cell concentrations (cells mL^{-1}) at $t = 0.5$ h. In those cultures, where no initial concentrations were measured (*Culture III* and *IV*, Table 1), the data were normalized indirectly (for details, see below).

From cell concentrations, daily specific growth rates $\mu_{24 \text{ h}}$ (d^{-1}) were derived as:

$$\mu_{24 \text{ h}} = \frac{\Delta \ln N}{\Delta t} = \frac{\ln N_t - \ln N_{t-24 \text{ h}}}{t - t_{-24 \text{ h}}} \quad (4)$$

where $N_{t-24 \text{ h}}$ and N_t represent the cultures' cell concentrations at the two consecutive sampling time points $t_{-24 \text{ h}}$ and t with a time lag of 24 h (Guillard 1973; Banse 1976; Wood et al.

2005). *Instantaneous* (relative) cell division rates $\text{Cell div}_{\text{rel}}$ (h^{-1}) were calculated as:

$$\text{Cell div}_{\text{rel}} = \frac{\Delta N_{\text{rel}}}{\Delta t_{1 \text{ h}}} = \frac{N_{\text{rel},t} - N_{\text{rel},t-1 \text{ h}}}{t - t_{-1 \text{ h}}} \quad (5)$$

where $N_{\text{rel},t-1 \text{ h}}$ and $N_{\text{rel},t}$ represent the cultures' relative cell concentrations at the two consecutive sampling time points $t_{-1 \text{ h}}$ and t sampled with a time lag of 1 h. Relative division rates (Eq. 5) can be converted to absolute cell division rates ($\text{cells mL}^{-1} \text{h}^{-1}$) by multiplying them with $N_{t_{0\text{h}}}$ (here approximated by $N_{t_{0.5 \text{ h}}}$).

Chl *a* concentrations were determined fluorometrically using a TD-700 fluorometer (Turner Designs, Sunnyvale, U.S.A.). Samples were taken by filtering defined volumes of cell culture onto glass fiber filters (Whatman, Maidstone, UK), which were instantly frozen in liquid nitrogen. Chl *a* was extracted in 90% acetone (v/v, Sigma, Munich, Germany) prior to the fluorometric measurements following the protocol by Holm-Hansen and Riemann (1978).

Concentrations of POC, PIC, and PON were measured with a Euro Vector CHNS-O elemental analyzer (Euro Elemental Analyser 3000, HEKAtech GmbH, Wegberg, Germany). Samples of total particulate carbon (TPC) and POC were taken by vacuum-filtration of defined volumes of culture onto precombusted glass fiber filters (15 h, 500°C) that were subsequently dried. For the quantification of POC, TPC filters were soaked with hydrochloric acid (0.2 mol L^{-1}) to remove any inorganic carbon. Concentrations of PIC were determined as the difference of TPC and POC concentrations.

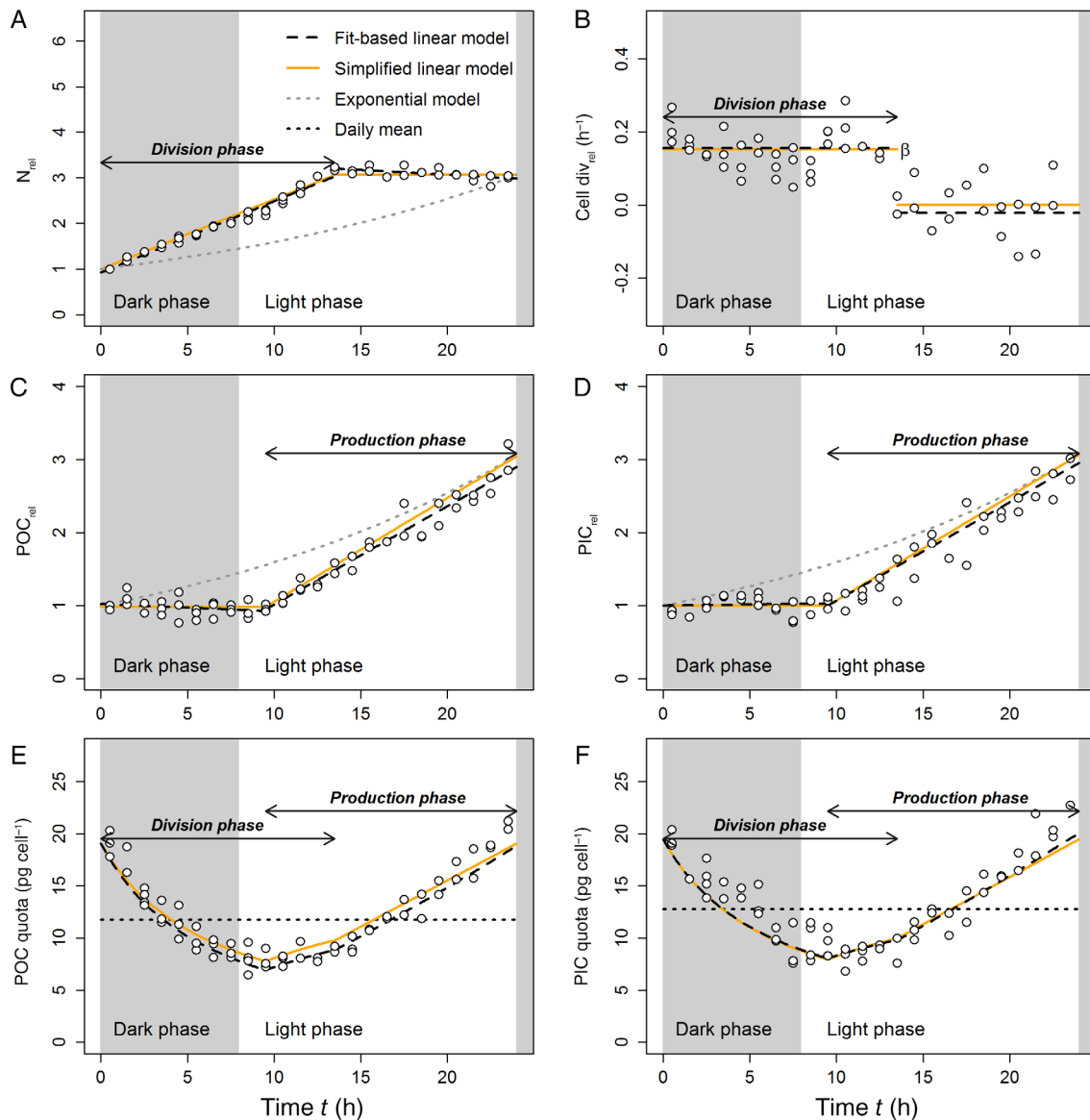


Fig. 2. Diel variations in cell parameters of the observed *E. huxleyi* culture. **(A)** Relative cell concentrations N_{rel} increase linearly during a 13.5 h *division phase* that starts at the beginning of the dark phase. The increase deviates from an exponential function on time scales < 24 h (cp. gray dotted curve). **(B)** Relative cell division rates $Cell\ div_{rel}$ are largely constant during the *division phase* (Eq. 10), but possess two recognizable maxima. **(C)** The cultures' relative POC concentrations POC_{rel} and **(D)** the relative PIC concentrations PIC_{rel} increase linearly during the 14.5 h *production phase* that starts 1.5 h after the beginning of the light phase. The increases deviate from exponential functions on time scales < 24 h (cp. gray dotted curves). Normalization of POC or PIC concentrations **(C, D)** to the respective cell concentrations **(A)** result in **(E)** cellular POC quotas (POC quota) and **(F)** cellular PIC quotas (PIC quota) that both strongly vary over the course of the day. Their daily means can be calculated according to equations given in Boxes 3, 4. [Color figure can be viewed at wileyonlinelibrary.com]

Because also the absolute values of POC and PIC concentrations differed between the cultures, concentrations were normalized to the initial POC and PIC concentrations. The resulting relative carbon concentrations, that is, relative POC and PIC concentrations (POC_{rel} and PIC_{rel} , dimensionless), are defined as:

$$POC_{rel} = POC_t / POC_{t_{0h}} \quad (6)$$

$$PIC_{rel} = PIC_t / PIC_{t_{0h}} \quad (7)$$

where POC_t and PIC_t represent the time-dependent POC and PIC concentrations of the different cultures ($pg\ mL^{-1}$) and $POC_{t_{0h}}$ and $PIC_{t_{0h}}$ represent the initial POC and PIC concentrations ($pg\ mL^{-1}$) at $t = 0.5$ h. Because in *Culture I* and *Culture II*, the scatter of the initial POC and PIC concentrations was high, we approximated the initial values by using the average of POC

and PIC concentrations over the dark phase instead. To emphasize the concept behind this normalization, we will, nevertheless, refer to these approximated values as “initial” in the following.

For the normalization of cell concentrations as well as POC and PIC concentrations (Eqs. 3, 6, 7), initial concentrations were unavailable for some of the cultures. This was because in *Culture III* and *V*, the dark phases were not sampled at all (Table 1), and in *Culture IV*, some of the data of the light phase was sampled prior to the dark phase (Table 1). In these cases, the data were normalized indirectly. For example, in *Culture III*, where no initial cell concentration was available, the data were normalized by dividing the absolute cell concentrations N_t by a correction factor CF:

$$CF = \frac{N_{III\ t_{6.5h}}}{(N_{rel\ I\ t_{6.5h}} + N_{rel\ II\ t_{6.5h}})/2} \quad (8)$$

This correction factor consists of the first available absolute cell concentration of *Culture III* here at $t = 6.5$ h ($N_{III\ t_{6.5h}}$, cells mL^{-1}), and the average over the relative cell concentrations of *Culture I* and *II* that are available at the same sampling time ($N_{rel\ I\ t_{6.5h}}$ is the relative cell concentration of *Culture I* at $t = 6.5$ h, and $N_{rel\ II\ t_{6.5h}}$ is the relative cell concentration of *Culture II* at $t = 6.5$ h).

Statistics:

Linear regressions were performed by application of the routine `lm()` using the software R (version 3.1.1 [2014], R Foundation for Statistical Computing, Vienna, Austria). Null hypotheses (slope is equal to zero) were rejected for p values smaller than 0.05.

Results:

Linear increase in cell concentrations during the dark and early light phase:

Cell concentrations of *E. huxleyi* increased linearly during the 8 h dark phase and in the first 5.5 h of the light phase (between $t = 0.5$ h and $t = 13.5$ h). They stayed relatively constant during the *late light phase* (between $t = 13.5$ h and $t = 23.5$ h; Fig. 2A). In the following, the period in which cell concentrations increased linearly is referred to as the *division phase* (defined as the period between $t = 0$ h and $t = 13.5$ h; see Fig. 3 for an overview of the different defined physiological phases). Linear regression of relative cell concentrations in the *division phase* yielded a slope β of $0.16 \pm 0.01 \text{ h}^{-1}$ ($R^2 = 0.98$, $n = 37$, $p < 2.2 \times 10^{-16}$ for two-sided t -test with null-hypothesis “slope = 0” Fig. 2A). Cell concentrations thus increased linearly at a constant rate of 0.16 times the initial cell concentration per hour. At the end of the *division phase* ($t = 13.5$ h), relative cell concentrations reached ≈ 3.1 , that is, cell concentrations had increased approximately threefold (Fig. 2A). A threefold increase in cell concentrations is well in line with the measured specific

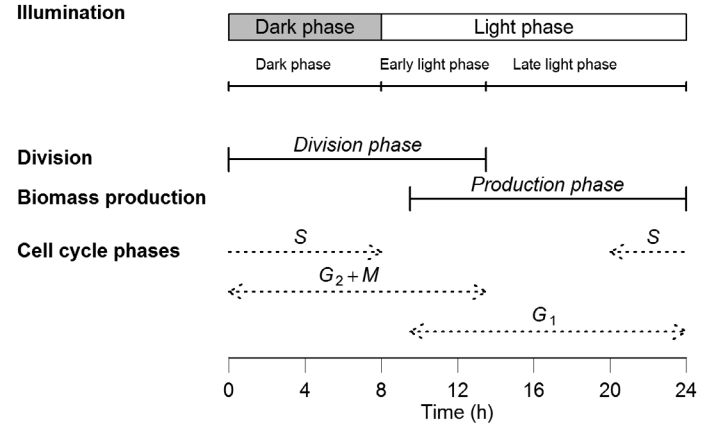


Fig. 3. Applied dark/light cycle and nomenclature for the resulting physiological phases. Cell cycle stages (cp. Fig. 1) are assumed based on the observed division and production patterns of this study (cp. Fig. 2).

growth rate of $\mu_{24\text{ h}} = 1.12 \text{ d}^{-1}$ that implies a daily multiplication of:

$$M_{24\text{ h}} = e^{\mu_{24\text{ h}} \cdot 24\text{ h}} = e^{1.12} = 3.06 \quad (9)$$

In the *late light phase*, linear regression of relative cell concentrations revealed a slope γ of $-0.02 \pm 0.01 \text{ h}^{-1}$ ($R^2 = 0.38$, $n = 18$, $p = 0.004$), that is, a minor decrease in cell concentrations was recognizable that is potentially a result of mortality or noise (although p is smaller than 0.05, the coefficient of determination, R^2 , is relatively small indicating a large amount of unexplained variance; Fig. 2A).

Based on the outcome of the linear regressions, we derive the following linear model for the course in relative cell concentrations during the *division phase*:

$$N_{rel}(t) = 1 + \beta \cdot t \quad \text{for } 0 \text{ h} \leq t \leq 13.5 \text{ h} \quad (10)$$

Relative cell concentrations in the *late light phase* (Fig. 2A) can accordingly be expressed as:

$$N_{rel}(t) = 1 + \beta \cdot 13.5 \text{ h} + \gamma \cdot (t - 13.5 \text{ h}) \quad \text{for } 13.5 \text{ h} \leq t \leq 24 \text{ h} \quad (11)$$

The functions for relative cell concentrations (Eqs. 10, 11) can be converted to functions for absolute concentrations by multiplying them with the initial cell concentrations that are here approximated by $N_{t_{0.5h}}$.

To inspect differences between the regression-based estimates of the increase in relative cell concentrations ($= \beta$) and the actually measured rates of increase (i.e., the “relative cell division rates” according to Eq. 5), we plotted the measured rates against time (Fig. 2B). This revealed that, despite being relatively constant, measured division rates possessed two recognizable maxima: a first maximum in the early dark phase (at $t = 0.5$ h) and a second maximum at the beginning

of the *early light phase* at $t = 10.5$ h (Fig. 2B). In between the two maxima, cell division rates underwent a minimum at approximately $t = 7.5$ h (Fig. 2B). This showed that cell division rates were not perfectly constant, but apparently took place in two broad phases. In a *first division phase* (from approximately $t = 0.5$ h to $t = 7.5$ h), cell concentrations doubled ($N_{\text{rel}} \approx 2$ at $t = 7.5$ h). In a *second division phase* ($t = 7.5$ h to $t = 13.5$ h), relative cell concentrations increased to 3.1 ($N_{\text{rel}} \approx 3.1$), that is, $\approx 50\%$ of cells at the end the *first division phase*, divided again in the *second division phase* (Fig. 2B):

$$\frac{N_{\text{rel},t_{13.5\text{h}}} - N_{\text{rel},t_{7.5\text{h}}}}{N_{\text{rel},t_{7.5\text{h}}}} = \frac{3.06 - 2}{2} = 0.53 = 53\% \quad (12)$$

Both *division phases* were similar in lengths and in the absolute amount of division events, but a significantly smaller fraction of cells underwent division in the *second division phase*.

Linear increase in POC and PIC concentrations during the light phase:

POC and PIC concentrations of all *E. huxleyi* cultures stayed relatively constant throughout the dark phase and in the first 1.5 h of the light phase (between $t = 0.5$ h and $t = 9.5$ h; Fig. 2C,D). They then increased linearly for the rest of the light phase (between $t = 9.5$ h and $t = 23.5$ h; Fig. 2C,D). We will refer to the period with linear increases in POC and PIC concentrations as the *production phase* (defined as the period between $t = 9.5$ h and $t = 24$ h; Fig. 3). At the end of the *production phase*, relative POC and PIC concentrations both reached ≈ 3.0 (Fig. 2C,D). Thus, similar to the cell concentrations, the relative increases in POC and PIC concentrations were in line with $\mu_{24\text{h}}$ that suggests a daily multiplication of $M_{24\text{h}} = 3.06$ (cp. Eq. 9).

A linear regression of the relative POC concentrations in the period before the *production phase* (between $t = 0.5$ h and $t = 9.5$ h) revealed a slope δ_{POC} of $-0.01 \pm 0.01 \text{ h}^{-1}$ ($R^2 = 0.10$, $n = 27$, $p < 2.2 \times 10^{-16}$) and a linear regression of the relative PIC concentrations in the same period revealed a slope δ_{PIC} of $0.00 \pm 0.01 \text{ h}^{-1}$ ($R^2 < 0.01$, $n = 22$, $p = 0.72$). The slight apparent decrease in the culture's POC concentration, if not being a result of noise, would indicate that POC but not PIC concentrations slightly decreased at a rate of 0.01 times the initial POC concentration per hour (Fig. 2C). Based on the results of the linear regressions, we describe relative POC concentrations and relative PIC concentrations before the *production phase* as:

$$\text{POC}_{\text{rel}}(t) = 1 + \delta_{\text{POC}} \cdot t \quad \text{for } 0 \text{ h} \leq t \leq 9.5 \text{ h} \quad (13)$$

$$\text{PIC}_{\text{rel}}(t) = 1 + \delta_{\text{PIC}} \cdot t \quad \text{for } 0 \text{ h} \leq t \leq 9.5 \text{ h} \quad (14)$$

(Fig. 2C,D). The functions for relative POC and PIC concentrations (Eqs. 13, 14) can be converted to functions for absolute concentrations by multiplication with the initial POC

and PIC concentrations, here approximated by $\text{POC}_{t_{0.5\text{h}}}$ and $\text{PIC}_{t_{0.5\text{h}}}$, respectively.

For the *production phase* (between $t = 9.5$ h and $t = 24$ h), linear regression yielded a slope ϵ_{POC} of $0.13 \pm 0.01 \text{ h}^{-1}$ ($R^2 = 0.95$, $n = 29$, $p < 2.2 \times 10^{-16}$) for POC concentrations, and a slope ϵ_{PIC} of $0.13 \pm 0.01 \text{ h}^{-1}$ ($R^2 = 0.91$, $n = 28$, $p < 2.6 \times 10^{-16}$) for PIC concentrations. Thus, the culture's relative POC and PIC concentrations both increased linearly at largely constant rates of 0.13 times the initial concentrations per hour (Fig. 2C,D). The models for relative POC and PIC concentrations in the *production phase* accordingly are:

$$\text{POC}_{\text{rel}}(t) = 1 + \delta_{\text{POC}} \cdot 9.5 \text{ h} + \epsilon_{\text{POC}} \cdot (t - 9.5 \text{ h}) \quad \text{for } 9.5 \text{ h} \leq t \leq 24 \text{ h} \quad (15)$$

$$\text{PIC}_{\text{rel}}(t) = 1 + \delta_{\text{PIC}} \cdot 9.5 \text{ h} + \epsilon_{\text{PIC}} \cdot (t - 9.5 \text{ h}) \quad \text{for } 9.5 \text{ h} \leq t \leq 24 \text{ h} \quad (16)$$

Although the linear models suggest that relative increases of POC and PIC concentrations were relatively similar (both: 0.13 h^{-1}), PIC : POC ratios showed an apparent increase during the dark phase, and an apparent decrease during the light phase (Fig. 4A). This is supposedly because a small fraction of POC, but not PIC, was continuously respired, which is not resolved by the model. Small rates of POC respiration are also indicated in the small apparent decrease in the relative POC concentrations before the *production phase* ($\delta_{\text{POC}} = -0.01 \text{ h}^{-1}$). It is furthermore indicated by a small decrease of POC : PON ratios and POC : cell volume ratios during the dark phase, and a small increase during the light phase (Fig. 4B,C). Chl *a* : POC ratio, in turn, showed a small increase during the dark phase, and a small decrease during the light phase (Fig. 4D).

Cellular POC and PIC quotas strongly vary during the day:

Normalization of the measured POC and PIC concentrations to the respective measured cell concentrations provided the data of cellular POC and PIC quotas (here: pg cell^{-1}). Between the beginning of the dark phase and the beginning of the *production phase*, when cells divided but stopped producing, cellular POC quotas decreased strongly from ≈ 20 to $\approx 8 \text{ pg cell}^{-1}$ (between $t = 0.5$ h and $t = 9.5$ h; Fig. 2E) and cellular PIC quotas similarly decreased from ≈ 20 to $\approx 10 \text{ pg cell}^{-1}$ (Fig. 2F). Between the beginning of the *production phase* and the end of the *division phase*, the measured cellular POC quotas increased slightly from ≈ 8 to $\approx 9 \text{ pg cell}^{-1}$ (between $t = 9.5$ h and 13.5 h, Fig. 2E) and PIC quotas decreased slightly from ≈ 10 to $\approx 9 \text{ pg cell}^{-1}$ (Fig. 2E,F). In the *late light phase*, when cell division stopped and cells kept producing, cellular POC quotas increased strongly from $\approx 9 \text{ pg cell}^{-1}$ back to $\approx 20 \text{ pg cell}^{-1}$ (between $t = 13.5$ h and 23.5 h; Fig. 2E) and cellular PIC quotas increased similarly from ≈ 9 to $\approx 21 \text{ pg cell}^{-1}$ (Fig. 2F). Overall, maximal POC and PIC quotas were 2.5 times larger than the daily minimums. Diel variations in POC and PIC quotas were thus slightly smaller than the variations in

cell concentrations and the culture's PIC and POC concentrations because the *division phase* and the *production phase* partially overlapped.

The models describing the cellular POC and PIC quotas of our data set (POC quota (t) or PIC quota (t), pg cell⁻¹; Fig. 2E, F) are derived by dividing the linear functions for POC or PIC concentrations (Eqs. 13–16) by the linear functions for cell concentrations at the respective time interval (Eqs. 10, 11; for the calculations of the models, see Box 1). Figure 2E,F shows that these fit-based stepwise models both agree well with the measured data and show the same pronounced diel variations over the course of the day.

Discussion:

Phased division and production in *E. huxleyi*:

Cultivation of *E. huxleyi* under a regular 16:8 h light/dark cycle induced a phasing in the species' cell division, and in its POC and PIC production. *E. huxleyi* is well known to entrain its cell division to regular light/dark cycles and has been shown to mainly divide during dark phases. The timing and lengths of division phases, however, varies between studies and strains (Table 2; Nelson and Brand 1979; Linschooten et al. 1991; Jochem and Meyerdierks 1999; Müller et al. 2008). Van Bleijswijk et al. (1995) observed that only cultures with more than one average division per day ($\mu_{24h} > \ln[2] [= 0.69] \text{ d}^{-1}$) stretch their division into light phases (Table 2). This suggests that *E. huxleyi*, which is known to divide by binary fission and can therefore only divide once within one DNA replication-division sequence, adds another DNA replication-division sequence in order to divide more than once per day (for reviews on cell division in microalgae, see Chisholm et al. 1984; Vaultot 1995; and Zachleder et al. 2016). When the dark phase is shorter than the length of two division sequences, cell division inevitable extends into the light phase. However, other studies observed division patterns where *E. huxleyi* with $\mu_{24h} < 0.69 \text{ d}^{-1}$ also partially divided in light phases (Table 2). Thus, stretched *division phases* may also occur when cellular division processes are generally slowed-down, for example, due to limiting resources (e.g., nutrients or light).

The long *division phase* with a linear increase in cell concentrations (Fig. 2A) implies that any cell cycle synchronization was only partial, otherwise cells would have increased in one or two sharp division peaks rather than at almost constant rates. Studies on *E. huxleyi* describing the relationship between light/dark cycles and cell cycle showed that cultures with approximately one division per day ($\mu_{24h} \approx 0.69 \text{ d}^{-1}$) pass into the S phase at the beginning of the dark phase. After a couple of hours, they change into the G₂+M phase, carrying out mitosis and cytokinesis. At the beginning of the next light phase, reach the G₁ phase, performing photosynthesis and calcification (van Bleijswijk and Veldhuis 1995; Jochem and Meyerdierks 1999). In our dataset, approximately 50% of the cells that divided once, divided again in the second *division*

phase (Eq. 12; Fig. 2B). We assume that these cells pass through two consecutive repetitions of the S and G₂+M sequence instead of directly returning to G₁ (Fig. 1). The decision whether a cell divides once or twice presumably depends on the cell volume that is critical for division (Müller et al. 2008; Zachleder et al. 2016). Cell volumes can be influenced by the rates of photosynthesis during the previous light phase (i.e., growth conditions such as light intensity) or by the length of this light phase.

The relatively linear increase in the culture's relative PIC and POC concentrations throughout the *production phase* implies that the cultures' POC and PIC production rates stayed relatively constant with time, although certain small-scale diel variations may not be resolved by the linear model (Fig. 4C, D). Relatively constant POC production rates from the beginning of the *production phase* came along with a relatively continuous increase in PON- and cell-volume normalized POC contents, and a continuous decrease in Chl *a* : POC ratios (Fig. 4). Given that POC and PIC production have previously been associated with G₁, it is likely that all the detected production in the early *production phase* was carried out by the fraction of cells that were already in G₁ (Linschooten et al. 1991; van Bleijswijk and Veldhuis 1995; Jochem and Meyerdierks 1999; Müller et al. 2008).

Cell-normalized POC and PIC concentrations (i.e., cellular POC and PIC quotas) only underwent small changes in the early *production phase* because the decrease in cellular POC and PIC quotas due to division approximately equaled the increase in cellular POC and PIC quotas due to photosynthesis or calcification, respectively (Fig. 2E,F). This shows that changes in cell quotas, when division is ongoing, cannot provide information about cellular production rates, because the production is "masked" by cell division. Cellular production only becomes visible from cell quotas after cell division has stopped. In our study, the increase in cellular POC and PIC quotas became linear in the *late light phase* (Fig. 2A). This implies that cell-normalized POC and PIC production stayed relatively constant during this period.

Rates of the cultures' relative POC production and PIC production were similar in magnitude (ϵ_{POC} and ϵ_{PIC} were equal, Eqs. 15, 16). Similar relative rates are also reflected in relatively constant PIC : POC ratios, which may explain why PIC : POC ratios stood out as particularly robust ecophysiological indicators in coccolithophores in the past (Fig. 4A; Paasche 2001; Raven and Crawford 2012; Meyer and Riebesell 2015; Feng et al. 2016). The small diel variations in PIC : POC, POC : PON, POC : cell volume, and Chl *a* : POC yet indicate that small parts of POC were respired (Fig. 4; assuming that the slope δ_{POC} of -0.01 represents the reality, approximately $\frac{0.01 \text{ h}^{-1} \cdot 24 \text{ h}}{0.13 \text{ h}^{-1} \cdot (24 \text{ h} - 9.5 \text{ h})} = 8.5\%$ of POC that was buildup over a course of a day was respired). To compensate for the respirational losses during the dark phase, relative POC production rates during the *production phase* presumably slightly exceeded the

Table 2. Summary of cell division patterns observed in *E. huxleyi* cells when cultures were grown under diel light/dark cycles.:

Division patterns	Light/dark cycle (h:h), T, light	$\mu_{24\text{ h}}$	Strains	Measured parameters	Authors
4–6 h <i>division phase</i> during late dark phase	7:17/10:14/14:1/18:6/16:8, 21°C; 0.07–0.11 cal cm ⁻² min ⁻¹	0.69 d ⁻¹	NA	Relative cell concentrations	Paasche (1967)
16–18 h <i>division phase</i> in all strains, starting at the beginning of dark phase, continuing for 6–8 h during light phase	14:10, 20°C; 5 × 10 ⁻² ly min ⁻¹	NA	BT6, MCH451B, C4, 92A, WHA	Short-term specific growth rates	Nelson and Brand (1979)
4 h <i>division phase</i> during early dark phase	16:8, 18°C; 90 μE m ⁻² s ⁻¹	NA	NA	Cellular PIC quotas	Linschooten et al. (1991)
<70 μmol photons m ⁻² s ⁻¹ ; division during the dark phase	16:8, 10°C/15°C; varying light intensities	<70 μmol photons m ⁻² s ⁻¹ ; 0.05–0.7 d ⁻¹ ≥70 μmol photons m ⁻² s ⁻¹ ; 0.7–0.9 d ⁻¹	Ch24–90 Ch25–90	Differentiation of cell cycles by DNA staining	van Bleijswijk et al. (1994)
≥70 μmol photons m ⁻² s ⁻¹ ; 1.2–16 h <i>division phase</i> starting 2–4 h before dark phase, continuing for 2–4 h during light phase	16:8, 10°C/15°C; light: NA	0.42 d ⁻¹	Natural population	Differentiation of cell cycles by DNA staining	van Bleijswijk and Veldhuis (1995)
10 h <i>division phase</i> , starting at middle of dark phase, continuing for 4 h during light phase	14:10, 18°C; 80 μE m ⁻² s ⁻¹	—	NA	Differentiation of cell cycles by DNA staining, forward angle light scatter	Jochem and Meyerliers (1999)
≈8 h <i>division phase</i> , starting ≈2 h after beginning of dark phase, continuing for ≈4 h during light phase	12:12, 21°C; 300 μmol photons m ⁻² s ⁻¹	1.05 d ⁻¹	CCMP 371	Relative cell concentrations; cell diameters	Müller et al. (2008)
≈11 h <i>division phase</i> , starting ≈2 h after beginning of dark phase, stopping ≈2 h before the end of the dark phase	16:8, 15°C; 195 μmol photons m ⁻² s ⁻¹	1.12 d ⁻¹	RCC 1216	Relative cell concentrations	This study
13.5 h <i>division phase</i> starting at beginning of dark phase, finishing 5.5 h after beginning of light phase					

relative PIC production rates, which is not resolved by the model (Fig. 2C,D).

Diel variations in division and production require alternative estimates of ecophysiological responses:

In ecophysiological studies, cell characteristics are often interpreted on the level of growth rates $\mu_{24\text{ h}}$ (Eq. 4), cellular pool sizes (e.g., cellular POC and PIC quotas), or production rates (e.g., cellular POC and PIC production rates) that are measured *at one time point of the day* only (Raven and Crawford 2012; Meyer and Riebesell 2015; Feng et al. 2016). Our data illustrate that determination of $\mu_{24\text{ h}}$ is hardly influenced by the time of day chosen for sampling when cell increments are measured after the end of the *division phase* (where cell concentrations are relatively constant; Fig. 2A). However, when a cell sample is taken during the *division phase*, it is very important to stick to 24 h periods, otherwise the rapid changes in cell concentration can easily lead to an over- or underestimation of $\mu_{24\text{ h}}$.

In agreement with earlier studies (e.g., Zondervan et al. 2002), our data show that cellular POC and PIC quotas of phytoplankton with phased division and production strongly vary over the course of the day. Here, maximal POC and PIC quotas were 2.5 times larger than the daily minimums, but the magnitudes of diel variations depend on overall growth ($\mu_{24\text{ h}}$) and on how strongly division and production phases overlap (Fig. 2E,F). Depending on the sampling time, these variations can lead to deviations of measured values from the daily mean. When a cellular POC quota is measured shortly after the onset of the light phase, the daily mean would be underestimated by approximately 33% in our example (Fig. 2E). When is measured at the end of the light phase, it would be overestimated by approximately 66% (Fig. 2E). Only measuring the POC quota approximately in middle of the *production phase*, the measured value would equal the daily mean (Fig. 2E; for details on the calculations of the daily mean, see below). This indicates that measurements of cellular pool sizes in the middle of the light phase, deliver good approximations of the daily mean. The exact time point at which the measured values equal the mean may, however, vary between experiments.

Besides the impact on measured absolute pool sizes, diel variations in cultures with phased division and production can under some circumstances introduce false positive or false negative “effects” of treatments, that is, they can lead to the detection of apparent changes in cellular pool sizes in response to a treatment that are artifacts of sampling times (Fig. 5A). False positive or negative effects can be introduced when two differently treated cultures are measured at *different times* of the day. This effect can be large even when sampling times are only different by a couple of hours (POC quotas measured at taken at $t = 15.5\text{ h}$, in our example, are almost 20% smaller than POC quotas measured at $t = 17.5\text{ h}$; Fig. 2E). Additionally, a false effect can be introduced when two

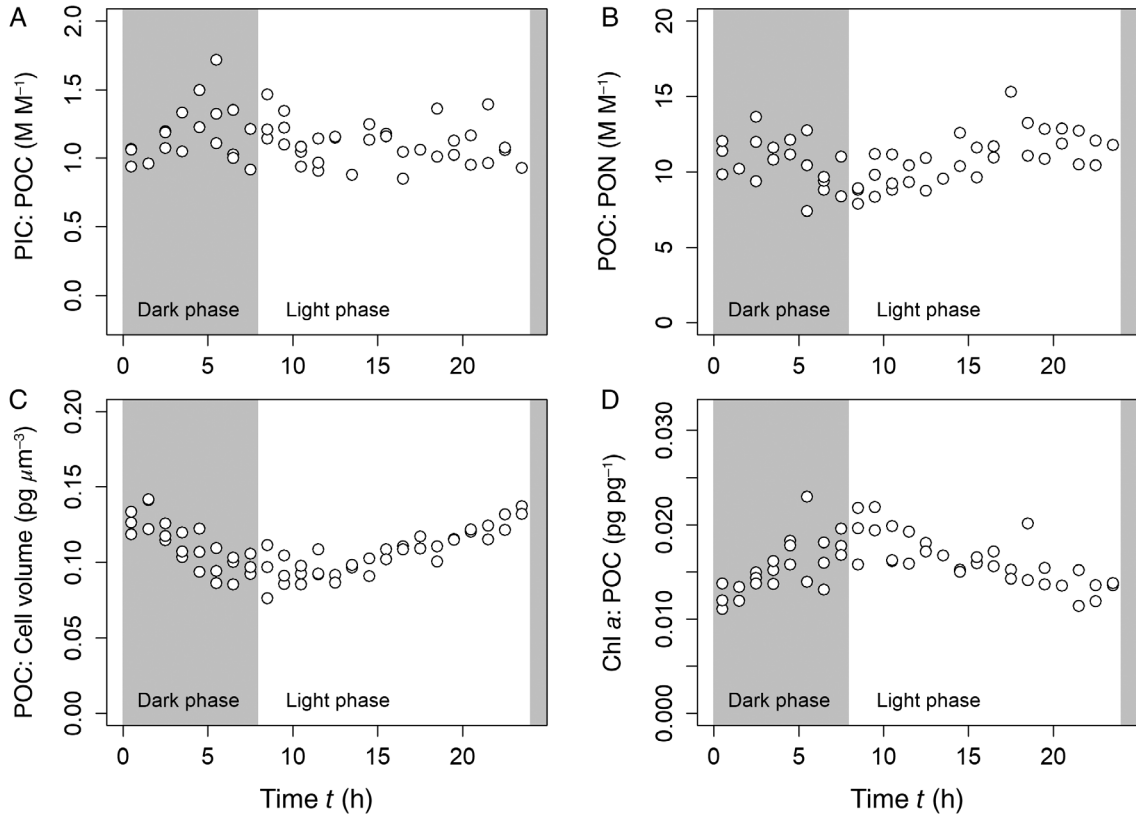


Fig. 4. Diel variations in cell stoichiometry. **(A)** PIC : POC ratios, **(B)** POC : PON ratios, **(C)** POC : cell volume ratios, and **(D)** Chl *a* : POC ratios. Diel variations are apparent in all presented parameters, but they are less pronounced than in cellular POC and PIC quotas (cp. Fig. 2E,F).

cultures are sampled at the *same time* of the day, because treatment-driven differences in cellular pool sizes vary over the course of the day if $\mu_{24\text{h}}$ has changed in response to the treatment (Fig. 5A). These types of errors are generally smaller, but can nevertheless affect the results. In the example in Fig. 5, two different treatments (e.g., high and low temperature) lead to a difference in $\mu_{24\text{h}}$ (between *Culture A* and *Culture B*). The daily means of the cultures' cellular POC quotas are meanwhile unaffected by the applied treatments. Although the mean POC quotas are equal under both growth conditions, an apparent increase in the POC quota of *Culture B* would be estimated if both cultures were sampled in the morning, and an apparent decrease in the POC quota would be estimated if the cultures were sampled in the evening (Fig. 5A).

Errors resulting from diel variations in rates of division and production go beyond cellular pool sizes, but also affect production rates of cellular biomass (in the following, we will explain this at the example of POC; Fig. 5B). This is not only because the biases in estimates of cellular production rates are similar to the above-described biases in estimates of cellular pool sizes (Fig. 5B), but also because conventional measures for cellular production rates do not account for short-term deviations from exponential growth. Cellular production rates are conventionally obtained as the product of a cellular pool size and the

specific growth rate $\mu_{24\text{h}}$ (Guillard 1973; Banse 1976; Wood et al. 2005):

$$\text{POC prod}_{\text{cell,conventional}} = \text{POC quota} \cdot \mu_{24\text{h}} \quad (17)$$

This equation derives from cultures in which cell division events and biomass production are evenly distributed over the day because the cells undergo their cell cycles in a fully unsynchronized manner. Such *continuous* growth can only occur when phytoplankton cultures are grown under constant light (Brand and Guillard 1981; Jochem and Meyerdierks 1999). In continuously growing cultures, both concentrations of cells and concentrations of biomass increase exponentially (at the same relative rates) over the course of the day (Fig. 6A,B):

$$N(t)_{\text{cont}} = N_{t_{0\text{h}}} \cdot e^{\mu_{24\text{h}} \cdot t} \quad (18)$$

$$\text{POC}(t)_{\text{cont}} = \text{POC}_{t_{0\text{h}}} \cdot e^{\mu_{24\text{h}} \cdot t} \quad (19)$$

The rates of increase of the culture's cell concentrations (i.e., the culture's division rates) and of biomass (i.e., the culture's biomass production rates) can be described by the derivative functions of Eqs. 18, 19, respectively:

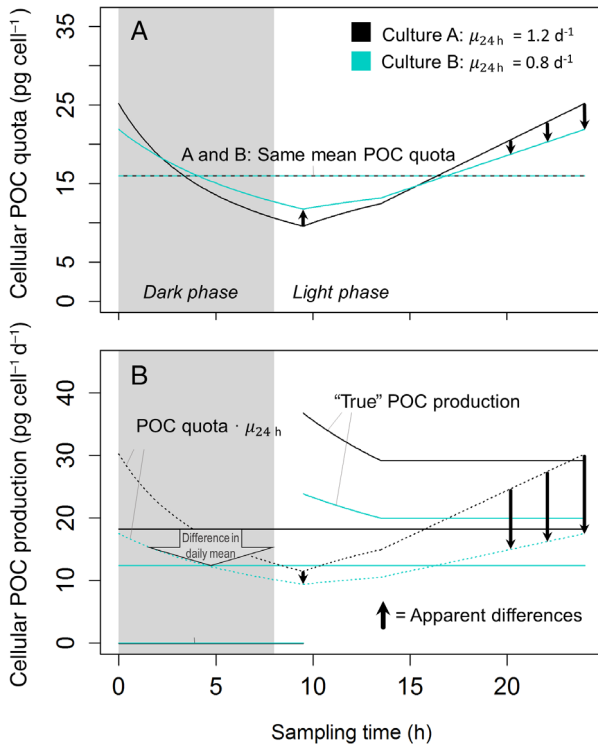


Fig. 5. Modeled consequences of phased division and production for the determination of physiological responses towards changing environmental conditions. **(A)** Modeled time-dependent cellular POC quotas of two *Cultures A* and *B* with different growth rates ($\mu_{24\text{ h}}$), but equal daily means in cellular POC quotas (horizontal line; cp. Box 5). **(B)** Modeled “true” time-dependent cellular POC production rates of the same cultures and their daily means (horizontal line) vs. apparent cellular production rates according to conventional methods ($\mu_{24\text{ h}} \cdot \text{POC quota}$; dotted curves). In order to have equal daily means of cellular POC quotas in *Culture A* and *B*, different initial POC quotas were chosen as model inputs. For more details, refer “Discussion” section. [Color figure can be viewed at wileyonlinelibrary.com]

$$N \text{ prod}(t)_{\text{cont}} = N'(t)_{\text{cont}} = N(t)_{\text{cont}} \cdot \mu_{24\text{ h}} \quad (20)$$

$$\text{POC prod}(t)_{\text{cont}} = \text{POC}'(t)_{\text{cont}} = \text{POC}(t)_{\text{cont}} \cdot \mu_{24\text{ h}} \quad (21)$$

These functions are exponential as well, that is, the culture’s division and biomass production rates increase exponentially with time.

Normalizing the function for the culture’s biomass concentration (Eq. 19) to the function of the respective cell concentrations (Eq. 18), one obtains *constant* cellular biomass quotas because the term $e^{\mu_{24\text{ h}} \cdot t}$ cancels out (Fig. 6C):

$$\begin{aligned} \text{POC quota}(t)_{\text{cont}} &= \frac{\text{POC}(t)_{\text{cont}}}{N(t)_{\text{cont}}} = \frac{\text{POC}_{t_{0\text{h}}} \cdot e^{\mu_{24\text{ h}} \cdot t}}{N_{t_{0\text{h}}} \cdot e^{\mu_{24\text{ h}} \cdot t}} \\ &= \frac{\text{POC}_{t_{0\text{h}}}}{N_{t_{0\text{h}}}} = \text{POC quota}_{t_{0\text{h}}} \end{aligned} \quad (22)$$

Normalizing the function for the culture’s biomass production rates (Eq. 21) to the respective function for cell concentrations

(Eq. 18), one obtains the well-known expression for the cellular biomass production rates (cp. Eq. 17) that is also constant:

$$\begin{aligned} \text{POC prod}_{\text{cell,cont}}(t) &= \frac{\text{POC}'_{\text{cont}}(t)}{N(t)_{\text{cont}}} = \frac{\text{POC}_{t_{0\text{h}}} \cdot e^{\mu_{24\text{ h}} \cdot t} \cdot \mu_{24\text{ h}}}{N_{t_{0\text{h}}} \cdot e^{\mu_{24\text{ h}} \cdot t}} \\ &= \text{POC quota}_{t_{0\text{h}}} \cdot \mu_{24\text{ h}} \end{aligned} \quad (23)$$

Because both, pools sizes and production rates of cellular compounds, are constant in continuously growing cultures, any sample taken intrinsically expresses the *daily mean* and is therefore comparable to the results of other studies (Shi et al. 2009; Müller et al. 2017).

In cultures with *phased* division and production, the “conventional” calculation of cellular production rates (Eqs. 17, 23) is, however, not valid. Applying it, neglects that the increase in cell and biomass concentrations differs from an exponential function on time scales $< 24\text{ h}$ (i.e., growth is not defined by $\mu_{24\text{ h}}$ and Eqs. 17–23 do not apply) and that cell and biomass increase in different periods of the day (Fig. 6). Consequently, cellular production rates of cultures with phased division and production have to be calculated differently than in continuous cultures. The correct way is to divide the nonexponential function describing the culture’s production rates of cellular components (in our data set, the derivative functions of Eqs. 13/15 multiplied with $\text{POC}_{t_{0\text{h}}}$ or the derivative functions of Eqs. 14/16 multiplied with $\text{PIC}_{t_{0\text{h}}}$) by the nonexponential function describing the respective cell concentrations (in our data set, to Eqs. 10/11 multiplied with $N_{t_{0\text{h}}}$; for details, refer to Box 2). The exact functions may thereby vary between phytoplankton species/strains and experiments, because division and production patterns can significantly differ (e.g., Table 2).

Figure 5B illustrates the resulting time-specific cellular POC production at the example of a notional culture with the same division and production pattern as observed in our dataset. From the example in Fig. 5, it becomes apparent that the “true” cellular POC production rates (according to Box 2) decrease slightly at the beginning of the *production phase* and then stay constant during the later *production phase*. It is also visible that the apparent cellular POC production rates (according to Eqs. 17, 23) undergo strong diel changes over the course of the day that are proportional with the POC quotas, even though the “true” cellular production rates are constant in the later *production phase*. Applying the “conventional” equation here (Eqs. 17/21) would consequently introduce significant errors to the estimates of production rates. In the presented *Culture A* and *Culture B*, the “true” production rates are more than twice as large as suggested by “conventional” measures at the beginning of the *production phase*, and are relatively similar to the actual production at the end of the *production phase* (Fig. 5B). Regarding daily means, the “conventional” equation would underestimate the mean by up to 30–40% when samples are taken at the beginning or the

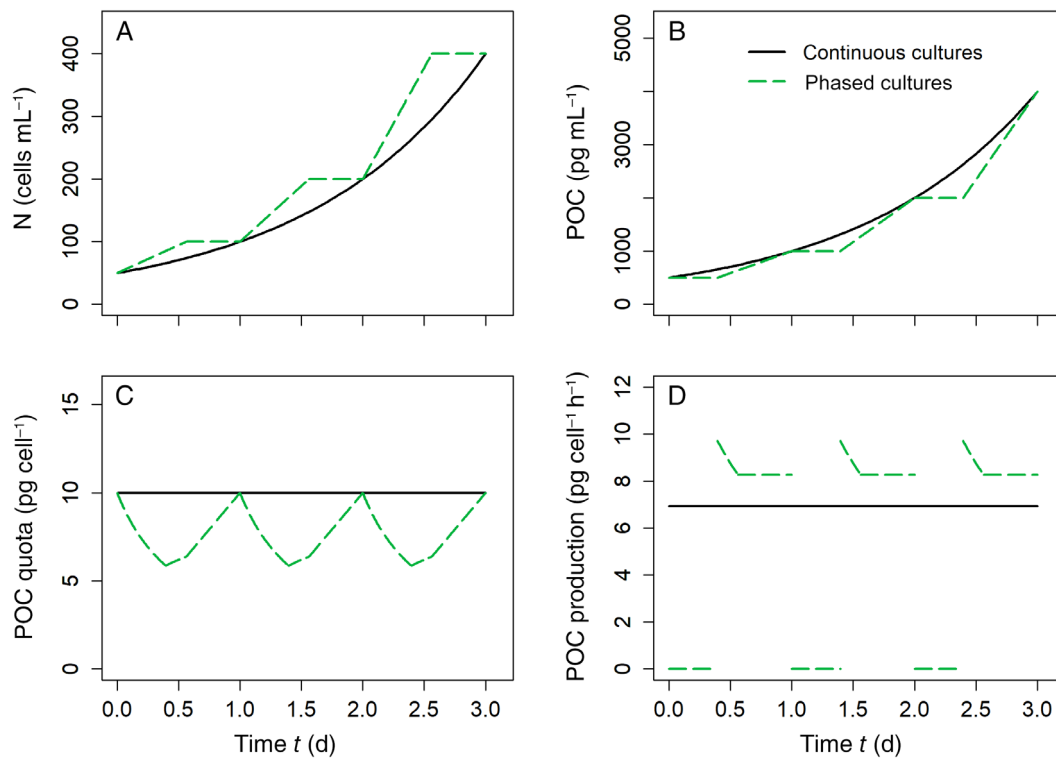


Fig. 6. Modeled differences between phytoplankton cultures with continuous vs. phased division and production. **(A)** Cell concentrations of continuously dividing cultures increase exponentially throughout the day, whereas the increase in cultures with phased division differs from exponential growth. **(B)** POC concentrations of continuously producing cultures increase exponentially throughout the day, whereas the increase in cultures with phased production differs from exponential growth. **(C)** Cellular POC quotas stay constant when both, cell division and POC production, are continuous. When division or production are phased, cellular POC quotas vary over the course of the day. **(D)** The cellular POC production is constant in continuously growing cultures, but shows diel variations in cultures with phased division/production. Models for continuous cultures are based on Equations 18–24. Models for the culture with phased division/production are based on the equations given in Box 5, assuming a 13.5 h *division phase* starting at $t = 0$ h, and a 14.5 h *production phase*, starting at $t = 9.5$ h. Both models use the same growth rate $\mu_{24 \text{ h}}$ and the same initial cell and POC concentrations, which results in different daily means of the POC quota. [Color figure can be viewed at wileyonlinelibrary.com]

end of the *production phase*, and would equal the mean approximately in the middle of the *production phase* (Fig. 5B).

Implications for the interpretation of existing research:

The entrainment of cell division to diel light/dark cycles is a well-described phenomenon that has been observed in most phytoplankton taxa (e.g., Marra 1978; Nelson and Brand 1979; Chisholm and Brand 1981; Harding et al. 1981). In most phytoplankton, cell division primarily takes place in dark phases, whereas biosynthesis naturally occurs in light phases. This temporal separation of cell division and biomass production can avoid the competition for energy resources or metabolic precursors, and give selective advantages with regards to nutrient acquisition or grazing pressure (Nelson and Brand 1979; Chisholm et al. 1984). Division patterns can, however, greatly differ between taxa and species. In diatoms, cell division is less strictly tied to the light/dark cycle. Cell division here often takes place with several peaks throughout the day and is frequently more pronounced during the light phase (Jorgensen 1966; Paasche 1968; Nelson and Brand 1979; Chisholm and Costello 1980; Yoder et al.

1982). Furthermore, division patterns can vary within the same species, because division patterns can depend on culture conditions and genomic variations (Table 2; Paasche 1967; Nelson and Brand 1979; Brand and Guillard 1981; Chisholm et al. 1984; Zachleder et al. 2016). Although division patterns can significantly vary, all cultures with phased division or phased production have in common that the increase in cell or biomass concentrations cannot be described by exponential functions on time scales < 24 h (i.e., Eqs. 18–23 are not valid). Furthermore, division and production occur in different periods of the day, resulting in diel variations of pool sizes and production rates of cellular components. Therefore, problems with respect to the diel fluctuations do not only apply to *E. huxleyi*, but at least to a certain degree, to all other phytoplankton.

To address how ecophysiological responses of phytoplankton cultures with phased division and production could be assessed in the future, it is to be discriminated whether the interest is in the cellular performance at a specific time point or whether the interest is in a daily average. A time-specific cellular quota or stoichiometric ratio can directly be obtained

from the respective sample. In the case of physiological rates (e.g., an instantaneous photosynthetic rate), time-specific measures can either be assessed by tracer incubation or gas exchange measurements (e.g., Marra 1978; Harding et al. 1981; Müller et al. 2008; Halsey et al. 2010, 2011) or they can be estimated from two consecutive biomass concentrations (e.g., POC concentrations) rather than from the product of a cellular quota and the specific growth rate (cp. Eqs. 17, 23):

$$\text{POC prod}_{\text{cell,inst}} = \frac{\Delta \text{POC}}{\Delta t \cdot N} \quad (24)$$

ΔPOC represents the difference of POC concentrations between two successive sampling times t (with a time delay no more than a few hours) and N is the cell concentration at the first sampling time. We discussed above that changes in cell quotas, when division is ongoing, cannot provide information about the rates of cellular biomass production, because the production is “masked” by cell division. Equation 24 makes the instantaneous cellular POC production “visible” because it takes into account changes in biomass concentrations but not cell concentrations.

Daily means in cellular pool sizes and production rates are more general measures that express the physiological performance of a culture independently of its current physiological state (and independently of the cell cycles in which a majority of the cells are at a given time). They are therefore comparable between experiments. One suggested approach to obtain daily means in cellular pool sizes and production rates is to fully desynchronize phytoplankton cultures by applying continuous light, in which case any sample taken intrinsically represents the daily mean (Jochem and Meyerdierks 1999; Shi et al. 2009; Müller et al. 2017). This approach is straight-forward, but it can only be applied when the observed phytoplankton truly desynchronizes in response to continuous light, and when its growth is unaffected by this treatment (Brand and Guillard 1981; Chisholm and Brand 1981; Bretherton et al. 2019).

We here propose analytical equations for the calculation of mean cellular pool sizes and production rates that are based on the integrals of the functions expressing time-dependent cellular pool sizes and production rates (Box 3, 4). All models presented in this publication, and the equations for the daily means of cultures with various division patterns, are implemented in a calculation sheet that we provide in the Supporting information. The calculations require sufficient knowledge of the diel division and production patterns of the investigated culture, that is, they have to be sampled prior to an experiment. Our calculations are only applicable to cultures in which the increases in cell and biomass concentrations can be approximated with linear models, and in which cell division events start at the beginning of the dark phase or is continuous (Box 3, 4; Supporting Information). If division or production patterns are different from that, the calculations would first have to be adjusted accordingly.

Input parameters for the suggested calculations of the means are the slopes of the linear functions describing the changes in cell and biomass concentrations over the course of the day. Because these slopes change with changing $\mu_{24 \text{ h}}$, sampling these parameters for every applied growth conditions would be very tedious. In order to reduce sampling effort, we suggest to estimate these slopes based on the measured $\mu_{24 \text{ h}}$ and the given lengths of the *division* and *production phase* (Box 5, Supporting Information). Once the division patterns (including the lengths of the division and production phases) have been presampled, $\mu_{24 \text{ h}}$ and one daily measurement of a cellular pool size as well as its sampling time are the only three input parameters for the calculations of the daily means (Box 5, Supporting Information). Figure 2 illustrates that the representation of the data by the “simplified” models (in orange) is similar to the representation by the fit-based models. However, due to the small continuous respiration of POC, “simplified” models overestimate relative POC concentrations and cellular POC quotas slightly (Fig. 2). When cell mortality or respiration are significant, these loss parameters have therefore to be accounted for in the model (for details, refer to the Calculation sheet provided in the Supporting Information).

Calculating the daily means, we were able to show that time-specific cellular pool sizes are often equal or similar to the mean approximately in the middle of a *production phase* (e.g., Fig. 5A). Also, time-specific apparent cellular production rates according to Eq. 23, despite being analytically wrong, consistently fluctuate around the daily mean and therefore often become equal to the mean approximately at the middle of a given *production phase* (e.g., Fig. 5B). This indicates that the large number of studies of the past that measured cell parameters at approximately midday still deliver good approximations of actual daily mean of cellular pool sizes and production rates. The exact time points when the time-dependent values equal the daily means, are however, different between pool sizes and apparent production rates (compare Fig. 5A with Fig. 5B). They furthermore vary with the cultures’ growth, production, respiration and mortality rates, and with the exact division and production patterns. These time points should therefore be identified before an experiment is sampled.

Summary and conclusions:

Here, we show that the increases in cell and biomass concentrations in *E. huxleyi* cultures with phased division and production on time scales < 24 h can be well described with stepwise linear functions. The deviations from exponential growth and the strong diel variations in cellular quotas implicate that cellular pool sizes and production rates calculated by conventional calculations can be erroneous. Errors with respect to cellular pool sizes and production rates due to sampling time can arise in all phytoplankton with phased division

or production and may have contributed to the variability in results of ecophysiological studies. Error sizes depend on sampling times (here, deviations from daily means were largest in the early and late light phase), the given phasing and production patterns (e.g., on whether *division phases* are very long or short, or on how strongly division and production overlap) and on overall growth (diel variations in pool sizes are typically larger, when μ_{24h} is large). To account for this, we suggest determining daily means, as opposed to time-specific physiological parameters. Daily means are comparable between studies and can be estimated by adjusting sampling times/experimental setups accordingly, or by using the analytical equations provided.

References:

- Banse, K. 1976. Rates of growth, respiration and photosynthesis of unicellular algae as related to cell size - a review. *J. Phycol.* **12**: 135–140. doi:10.1111/j.1529-8817.1976.tb00490.x
- Brand, L. E., and R. R. L. Guillard. 1981. The effects of continuous light and light intensity on the reproduction rates of twenty-two species of marine phytoplankton. *J. Exp. Mar. Biol. Ecol.* **50**: 119–132. doi:10.1016/0022-0981(81)90045-9
- Bretherton, L., and others. 2019. Day length as a key factor moderating the response of coccolithophore growth to elevated pCO₂. *Limnol. Oceanogr.* **64**: 1284–1296. doi:10.1002/lno.11115
- Chisholm, S. W., and J. C. Costello. 1980. Influence of environmental factors and population composition on the timing of cell division in *Thalassiosira fluviatilis* (*Bacillariophyceae*) grown on dark/light cycles. *J. Phycol.* **16**: 375–383. doi:10.1111/j.1529-8817.1980.tb03048.x
- Chisholm, S. W., and L. E. Brand. 1981. Persistence of cell division phasing in marine phytoplankton in continuous light after entrainment to light:dark cycles. *J. Exp. Mar. Biol. Ecol.* **51**: 107–118. doi:10.1016/0022-0981(81)90123-4
- Chisholm, S. W., D. Vaulot, and R. Olson. 1984. In L. N. Edmunds, Jr. [ed.], *Cell cycle clocks. Cell cycle controls in phytoplankton: Comparative physiology and ecology*. p. 365–394. Marcel Dekker, Inc., New York, doi:10.1104/pp.80.4.918
- Feng, Y., M. Y. Roleda, E. Armstrong, P. W. Boyd, and C. L. Hurd. 2016. Environmental controls on the growth, photosynthetic and calcification rates of a Southern Hemisphere strain of the coccolithophore *Emiliania huxleyi*. *Limnol. Oceanogr.* **62**: 519–540. doi:10.1002/lno.10442
- Guillard, R. R. 1973. Division rates. In Janet R. Stein [ed.], *Handbook of phycological methods: Culture methods and growth measurements*. p. 289–311. Cambridge University Press
- Guillard, R. R. L., and J. H. Ryther. 1962. Studies of marine planktonic diatoms I. *Cyclotella nana* Hustedt, and *Detonula confervacea* Cleve. *Can. J. Microbiol.* **8**: 229–239. doi:10.1139/m62-029
- Halsey, K. H., A. J. Milligan, and M. J. Behrenfeld. 2010. Physiological optimization underlies growth rate-independent chlorophyll-specific gross and net primary production. *Photosynth. Res.* **103**: 125–137. doi:10.1007/s11120-009-9526-z
- Halsey, K. H., A. J. Milligan, and M. J. Behrenfeld. 2011. Linking time-dependent carbon-fixation efficiencies in *Dunaliella tertiolecta* (Chlorophyceae) to underlying metabolic pathways. *J. Phycol.* **47**: 66–76. doi:10.1111/j.1529-8817.2010.00945.x
- Harding, L. W., B. W. Meeson, B. B. Prezelin, and B. M. Sweeney. 1981. Diel periodicity of photosynthesis in marine phytoplankton. *Mar. Biol.* **61**: 95–105. doi:10.1007/bf00386649
- Holm-Hansen, O., and B. Riemann. 1978. Chlorophyll a determination: Improvements in methodology. *Oikos* **30**: 438–447. doi:10.2307/3543338
- Hoogenhout, H. 1963. Synchronous cultures of algae. *Phycologia* **2**: 135–147. doi:10.2216/i0031-8884-2-4-135.1
- Howard, A., and S. R. Pelc. 1953. Synthesis of deoxyribonucleic acid in normal and irradiated cells and its relation to chromosome breakage. *Int. J. Radiat. Biol. Relat. Stud. Phys. Chem. Med.* **6**: 261–273. doi:10.1080/09553008514552501
- Jochem, F. J., and D. Meyerdierks. 1999. Cytometric measurement of the DNA cell cycle in the presence of chlorophyll autofluorescence in marine eukaryotic phytoplankton by the blue-light excited dye -1. *Mar. Ecol. Prog. Ser.* **185**: 301–307. doi:10.3354/meps185301
- Jorgensen, E. 1966. Photosynthetic activity during the life cycle of synchronous *Skeletonema* cells. *Physiol. Plant.* **19**: 789–799. doi:10.1111/j.1399-3054.1966.tb07065.x
- Linschooten, C., J. D. L. Bleijswijk, P. R. Emburg, J. P. M. Vrind, E. S. Kempers, P. Westbroek, and E. W. Vrind-de Jong 1991. Role of the light-dark cycle and medium composition on the production of coccoliths by *Emiliania huxleyi* (Haptophyceae). *J. Phycol.* **27**: 82–86. doi:10.1111/j.0022-3646.1991.00082.x
- MacIntyre, H. L., and J. J. Cullen. 2005. Using cultures to investigate the physiological ecology of microalgae, p. 287–326. In Robert A. Anderson [ed.], *Algal culturing techniques*. Elsevier: Academic Press. doi:10.1016/b978-012088426-1/50020-2
- Marra, J. 1978. Effect of short-term variations in light intensity on photosynthesis of a marine phytoplankton: A laboratory simulation study. *Mar. Biol.* **46**: 191–202. doi:10.1007/bf00390680
- Meyer, J., and U. Riebesell. 2015. Reviews and syntheses: Responses of coccolithophores to ocean acidification: A meta-analysis. *Biogeosciences* **12**: 1671–1682. doi:10.5194/bg-12-1671-2015
- Müller, M. N., A. N. Antia, and J. La Roche. 2008. Influence of cell cycle phase on calcification in the coccolithophore

- Emiliana huxleyi*. *Limnol. Oceanogr.* **53**: 506–512. doi:10.4319/lo.2008.53.2.0506
- Müller, M. N., T. W. Trull, and G. M. Hallegraeff. 2017. Independence of nutrient limitation and carbon dioxide impacts on the Southern Ocean coccolithophore *Emiliana huxleyi*. *ISME J.* **11**: 1777–1787. doi:10.1038/ismej.2017.53
- Nelson, D. M., and L. E. Brand. 1979. Cell division periodicity in 13 species of phytoplankton on a light:dark cycle. *J. Phycol.* **15**: 67–75. doi:10.1111/j.0022-3646.1979.00067.x
- Paasche, E. 1967. Marine plankton algae grown with light:dark cycles. I. *Coccolithus huxleyi*. *Physiol. Plant.* **20**: 946–956. doi:10.1111/j.1399-3054.1967.tb08382.x
- Paasche, E. 1968. Marine plankton algae grown with light-dark cycles. II. *Ditylum brightwellii* and *Nitzschia turgidula*. *Physiol. Plant.* **21**: 66–77. doi:10.1111/j.1399-3054.1968.tb07231.x
- Paasche, E. 2001. A review of the coccolithophorid *Emiliana huxleyi* (Prymnesiophyceae), with particular reference to growth, coccolith formation, and calcification-photosynthesis interactions. *Phycologia* **40**: 503–529. doi:10.2216/i0031-8884-40-6-503.1
- Prison, A., and H. Lorenzen. 1966. Synchronized dividing algae. *Annu. Rev. Plant Physiol.* **17**: 439–458. doi:10.1146/annurev.pp.17.060166.002255
- Raven, J., and K. Crawford. 2012. Environmental controls on coccolithophore calcification. *Mar. Ecol. Prog. Ser.* **470**: 137–166. doi:10.3354/meps09993
- Rost, B., and U. Riebesell. 2004. Coccolithophores and the biological pump: Responses to environmental changes, p. 76–99. *In* H. R. Thierstein and J. R. Young [eds.], *Coccolithophores - from molecular processes to global impact*. Springer. doi:10.1007/978-3-662-06278-4_5
- Shi, D., Y. Xu, and F. M. M. Morel. 2009. Effects of the pH/pCO₂ control method on medium chemistry and phytoplankton growth. *Biogeosciences*. **6**: 1199–1207. doi:10.5194/bg-6-1199-2009
- van Bleijswijk, J. D. L., and M. J. W. Veldhuis. 1995. In situ gross growth rates of *Emiliana huxleyi* in enclosures with different phosphate loadings revealed by diel changes in DNA content. *Mar. Ecol. Prog. Ser.* **121**: 271–277. doi:10.3354/meps121271
- van Bleijswijk, J. D., R. S. Kempers, M. J. Veldhuis and P. Westbroek, 1994. Cell and growth characteristics of types A and B of *Emiliana huxleyi* (Prymnesiophyceae) as determined by flow cytometry and chemical analyses. *J. Phycol.* **30**: 230–241. doi:10.1111/j.0022-3646.1994.00230.x
- Vaulot, D.. 1995. *In* I. Joint [ed.], *The Cell Cycle of Phytoplankton: Coupling Cell Growth to Population Growth*. *Molecular Ecology of Aquatic Microbes*. **38**: 303–322. Springer. doi:10.1007/978-3-642-79923-5_17
- Wood, A. M., R. Everroad, and L. Wingard. 2005. *In* Robert A. Andersen [ed], *Algal Culturing Techniques*. Measuring growth rates in microalgal cultures. *Algal Cult. Tech.* **18**: 269–288. Elsevier. doi:10.1016/b978-012088426-1/50019-6
- Yoder, J. A., J. Martin, and A. Nill. 1982. Cell division periodicity and the nitrate environment of a marine diatom. *Limnol. Oceanogr.* **27**: 352–357. doi:10.4319/lo.1982.27.2.0352
- Zachleder, V., K. Bišová, and M. Vítová. 2016. The cell cycle of microalgae, p. 3–46. *In* Borowitzka, A. Michael, Beardall, John, Raven A. John, [Eds.], *The physiology of microalgae*. Springer. doi:10.1007/978-3-319-24945-2_1
- Zondervan, I. 2007. The effects of light, macronutrients, trace metals and CO₂ on the production of calcium carbonate and organic carbon in coccolithophores - a review. *Deep-Sea Res. Part II Top. Stud. Oceanogr.* **54**: 521–537. doi:10.1016/j.dsr2.2006.12.004
- Zondervan, I., B. Rost, and U. Riebesell. 2002. Effect of CO₂ concentration on the PIC/POC ratio in the coccolithophore *Emiliana huxleyi* grown under light-limiting conditions and different daylengths. *J. Exp. Mar. Biol. Ecol.* **272**: 55–70. doi:10.1016/s0022-0981(02)00037-0

Acknowledgments:

We thank Lena Holtz, Glen Wheeler, Sebastian Rokitta, Gerald Langer, Nathan Christmas, Björn Rost, and Colin Brownlee for their helpful feedback on this manuscript. We also thank Christiane Lorenzen for measuring the elemental analyser samples. We acknowledge the constructive comments of the three anonymous reviewers. D.M.K. was funded by the European Research Council ERC-ADG-670390. S.T. was funded by the Federal Ministry of Education and Research (BMBF, ZeBiCa2 031A518C).

Conflict of Interest:

None declared.

Submitted 03 May 2019

Revised 06 November 2019

Accepted 08 January 2020

Associate editor: Ilana Berman-Frank

Box 1: Fit-based models for the time-dependent cellular POC quotas (pg cell^{-1}) and PIC quotas (pg cell^{-1}) of the observed *E. huxleyi* cultures.:

Prior to production phase:

$$\text{POC quota}(t) = \frac{\text{POC}(t)}{N(t)} = \frac{\text{POC}_{t_{0h}} \cdot (1 + \delta_{\text{POC}} \cdot t)}{N_{t_{0h}} \cdot (1 + \beta \cdot t)} = \text{POC quota}_{t_{0h}} \cdot \frac{1 + \delta_{\text{POC}} \cdot t}{1 + \beta \cdot t} \quad \text{for } 0 \text{ h} \leq t \leq 9.5 \text{ h} \quad (1.1)$$

$$\text{PIC quota}(t) = \frac{\text{PIC}(t)}{N(t)} = \frac{\text{PIC}_{t_{0h}} \cdot (1 + \delta_{\text{PIC}} \cdot t)}{N_{t_{0h}} \cdot (1 + \beta \cdot t)} = \text{PIC quota}_{t_{0h}} \cdot \frac{1 + \delta_{\text{PIC}} \cdot t}{1 + \beta \cdot t} \quad \text{for } 0 \text{ h} \leq t \leq 9.5 \text{ h} \quad (1.2)$$

Between start of production phase and end of division phase:

$$\begin{aligned} \text{POC quota}(t) &= \frac{\text{POC}(t)}{N(t)} = \frac{\text{POC}_{t_{0h}} \cdot (1 + \delta_{\text{POC}} \cdot 9.5 \text{ h} + \varepsilon_{\text{POC}} \cdot (t - 9.5 \text{ h}))}{N_{t_{0h}} \cdot (1 + \beta \cdot t)} \\ &= \text{POC quota}_{t_{0h}} \cdot \frac{1 + \delta_{\text{POC}} \cdot 9.5 \text{ h} + \varepsilon_{\text{POC}} \cdot (t - 9.5 \text{ h})}{1 + \beta \cdot t} \quad \text{for } 9.5 \text{ h} \leq t \leq 13.5 \text{ h} \end{aligned} \quad (1.3)$$

$$\begin{aligned} \text{PIC quota}(t) &= \frac{\text{PIC}(t)}{N(t)} = \frac{\text{PIC}_{t_{0h}} \cdot (1 + \delta_{\text{PIC}} \cdot 9.5 \text{ h} + \varepsilon_{\text{PIC}} \cdot (t - 9.5 \text{ h}))}{N_{t_{0h}} \cdot (1 + \beta \cdot t)} \\ &= \text{PIC quota}_{t_{0h}} \cdot \frac{1 + \delta_{\text{PIC}} \cdot 9.5 \text{ h} + \varepsilon_{\text{PIC}} \cdot (t - 9.5 \text{ h})}{1 + \beta \cdot t} \quad \text{for } 9.5 \text{ h} \leq t \leq 13.5 \text{ h} \end{aligned} \quad (1.4)$$

After end of division phase:

$$\begin{aligned} \text{POC quota}(t) &= \frac{\text{POC}(t)}{N(t)} = \frac{\text{POC}_{t_{0h}} \cdot (1 + \delta_{\text{POC}} \cdot 9.5 \text{ h} + \varepsilon_{\text{POC}} \cdot (t - 9.5 \text{ h}))}{N_{t_{0h}} \cdot (1 + \beta \cdot 13.5 \text{ h} + \gamma \cdot (t - 13.5 \text{ h}))} \\ &= \text{POC quota}_{t_{0h}} \cdot \frac{1 + \delta_{\text{POC}} \cdot 9.5 \text{ h} + \varepsilon_{\text{POC}} \cdot (t - 9.5 \text{ h})}{1 + \beta \cdot 13.5 \text{ h} + \gamma \cdot (t - 13.5 \text{ h})} \quad \text{for } 13.5 \text{ h} \leq t \leq 24 \text{ h} \end{aligned} \quad (1.5)$$

$$\begin{aligned} \text{PIC quota}(t) &= \frac{\text{PIC}(t)}{N(t)} = \frac{\text{PIC}_{t_{0h}} \cdot (1 + \delta_{\text{PIC}} \cdot 9.5 \text{ h} + \varepsilon_{\text{PIC}} \cdot (t - 9.5 \text{ h}))}{N_{t_{0h}} \cdot (1 + \beta \cdot 13.5 \text{ h} + \gamma \cdot (t - 13.5 \text{ h}))} \\ &= \text{PIC quota}_{t_{0h}} \cdot \frac{1 + \delta_{\text{PIC}} \cdot 9.5 \text{ h} + \varepsilon_{\text{PIC}} \cdot (t - 9.5 \text{ h})}{1 + \beta \cdot 13.5 \text{ h} + \gamma \cdot (t - 13.5 \text{ h})} \quad \text{for } 13.5 \text{ h} \leq t \leq 24 \text{ h} \end{aligned} \quad (1.6)$$

Models are derived by dividing the stepwise linear functions describing POC or PIC concentrations in the different time intervals (cp. Eqs. 13–16) by the respective stepwise linear functions describing cell concentrations in the same intervals (cp. Eqs. 10, 11). $\text{POC}_{t_{0h}}$, $\text{PIC}_{t_{0h}}$, and $N_{t_{0h}}$ are the POC (cells mL^{-1}), PIC (cells mL^{-1}), and cell concentrations (cells mL^{-1}) at the beginning of the dark phase. $\text{POC quota}_{t_{0h}}$ and $\text{PIC quota}_{t_{0h}}$ are the cellular POC quota (pg cell^{-1}) and PIC quota (pg cell^{-1}) at the beginning of the dark phase. t is the time of the day (h). δ_{POC} and δ_{PIC} are the slopes (h^{-1}) of the minor linear decrease in relative POC and PIC concentrations before the start of the *production phase*. ε_{POC} and ε_{PIC} are the slopes (h^{-1}) of the linear increase in relative POC and PIC concentrations during the *production phase*. β is the slope (h^{-1}) of the increase in relative cell concentrations during the *division phase*, and γ is the slope (h^{-1}) of the minor decrease in relative cell concentrations after the end of the *division phase*.

Box 2: Fit-based models for the time-dependent cellular POC production rates (POC prod_{cell}; pg cell⁻¹ h⁻¹) and cellular PIC production rates (PIC prod_{cell}; pg cell⁻¹ h⁻¹) of the observed *E. huxleyi* cultures.:

Prior to production phase:

$$\text{POC prod}_{\text{cell}}(t) = \frac{\text{POC}'(t)}{N(t)} = \frac{\text{POC}_{t_{\text{oh}}} \cdot \delta_{\text{POC}}}{N_{t_{\text{oh}}} \cdot (1 + \beta \cdot t)} = \text{POC quota}_{t_{\text{oh}}} \cdot \frac{\delta_{\text{POC}}}{1 + \beta \cdot t} \quad \text{for } 0 \text{ h} \leq t \leq 9.5 \text{ h} \quad (2.1)$$

$$\text{PIC prod}_{\text{cell}}(t) = \frac{\text{PIC}'(t)}{N(t)} = \frac{\text{PIC}_{t_{\text{oh}}} \cdot \delta_{\text{PIC}}}{N_{t_{\text{oh}}} \cdot (1 + \beta \cdot t)} = \text{PIC quota}_{t_{\text{oh}}} \cdot \frac{\delta_{\text{PIC}}}{1 + \beta \cdot t} \quad \text{for } 0 \text{ h} \leq t \leq 9.5 \text{ h} \quad (2.2)$$

Between start of production phase and end of division phase:

$$\text{POC prod}_{\text{cell}}(t) = \frac{\text{POC}'(t)}{N(t)} = \frac{\text{POC}_{t_{\text{oh}}} \cdot \varepsilon_{\text{POC}}}{N_{t_{\text{oh}}} \cdot (1 + \beta \cdot t)} = \text{POC quota}_{t_{\text{oh}}} \cdot \frac{\varepsilon_{\text{POC}}}{1 + \beta \cdot t} \quad \text{for } 9.5 \text{ h} \leq t \leq 13.5 \text{ h} \quad (2.3)$$

$$\text{PIC prod}_{\text{cell}}(t) = \frac{\text{PIC}'(t)}{N(t)} = \frac{\text{PIC}_{t_{\text{oh}}} \cdot \varepsilon_{\text{PIC}}}{N_{t_{\text{oh}}} \cdot (1 + \beta \cdot t)} = \text{PIC quota}_{t_{\text{oh}}} \cdot \frac{\varepsilon_{\text{PIC}}}{1 + \beta \cdot t} \quad \text{for } 9.5 \text{ h} \leq t \leq 13.5 \text{ h} \quad (2.4)$$

After end of division phase:

$$\begin{aligned} \text{POC prod}_{\text{cell}}(t) &= \frac{\text{POC}'(t)}{N(t)} = \frac{\text{POC}_{t_{\text{oh}}} \cdot \varepsilon_{\text{POC}}}{N_{t_{\text{oh}}} \cdot (1 + \beta \cdot 13.5 \text{ h} + \gamma \cdot (t - 13.5 \text{ h}))} \\ &= \text{POC quota}_{t_{\text{oh}}} \cdot \frac{\varepsilon_{\text{POC}}}{1 + \beta \cdot 13.5 \text{ h} + \gamma \cdot (t - 13.5 \text{ h})} \quad \text{for } 13.5 \text{ h} \leq t \leq 24 \text{ h} \end{aligned} \quad (2.5)$$

$$\begin{aligned} \text{PIC prod}_{\text{cell}}(t) &= \frac{\text{PIC}'(t)}{N(t)} = \frac{\text{PIC}_{t_{\text{oh}}} \cdot \varepsilon_{\text{PIC}}}{N_{t_{\text{oh}}} \cdot (1 + \beta \cdot 13.5 \text{ h} + \gamma \cdot (t - 13.5 \text{ h}))} \\ &= \text{PIC quota}_{t_{\text{oh}}} \cdot \frac{\varepsilon_{\text{PIC}}}{1 + \beta \cdot 13.5 \text{ h} + \gamma \cdot (t - 13.5 \text{ h})} \quad \text{for } 13.5 \text{ h} \leq t \leq 24 \text{ h} \end{aligned} \quad (2.6)$$

Models are derived by dividing the derivative functions (POC'(t); PIC'(t)) of the stepwise linear functions describing POC or PIC concentrations in the different time intervals (cp. Eqs. 13–16) by the respective stepwise linear functions describing cell concentrations in the same intervals (cp. Eqs. 10, 11). t is the time of the day (h). POC_{t_{oh}}, PIC_{t_{oh}}, and N_{t_{oh}} are the POC (cells mL⁻¹), PIC (cells mL⁻¹), and cell concentrations (cells mL⁻¹) at the beginning of the dark phase, respectively. POCquota_{t_{oh}} and PICquota_{t_{oh}} are the cellular POC quota (pg cell⁻¹) and PIC quota (pg cell⁻¹) at the beginning of the dark phase. δ_{POC} and δ_{PIC} are the slopes (h⁻¹) of the minor linear decrease in relative POC and PIC concentrations before the start of the *production phase*. ε_{POC} and ε_{PIC} are the slopes (h⁻¹) of the linear increase in relative POC and PIC concentrations during the *production phase*. β is the slope (h⁻¹) of the increase in relative cell concentrations during the *division phase*, and γ is the slope (h⁻¹) of the minor decrease in relative cell concentrations after the end of the *division phase*.

Box 3: Calculation of the daily mean of cellular pools sizes (pg cell⁻¹) of the observed *E. huxleyi* cultures at the example of POC.:

For $\gamma \neq 0$:

$$\text{POC quota}_{\text{mean}} = \frac{\text{POC quota}_{t_{\text{oh}}}}{24 \text{ h}} \cdot \left(\int_{0\text{h}}^{9.5\text{h}} \frac{1 + \delta_{\text{POC}} \cdot t}{1 + \beta \cdot t} dt + \int_{9.5\text{h}}^{13.5\text{h}} \frac{1 + \delta_{\text{POC}} \cdot 9.5 \text{ h} + \varepsilon_{\text{POC}} \cdot (t - 9.5 \text{ h})}{1 + \beta \cdot t} dt + \int_{13.5\text{h}}^{24\text{h}} \frac{1 + \delta_{\text{POC}} \cdot 9.5 \text{ h} + \varepsilon_{\text{POC}} \cdot (t - 9.5 \text{ h})}{1 + \beta \cdot 13.5 \text{ h} + \gamma \cdot (t - 13.5 \text{ h})} dt \right)$$

$$= \frac{\text{POC quota}_{t_{\text{oh}}}}{24 \text{ h}} \cdot \left(\begin{aligned} & \frac{(\beta - \delta_{\text{POC}}) \cdot \ln(9.5 \text{ h} \cdot \beta + 1) + \delta_{\text{POC}} \cdot 9.5 \text{ h} \cdot \beta}{\beta^2} \\ & + \frac{(\beta \cdot (1 + 9.5 \text{ h} \cdot (\delta_{\text{POC}} - \varepsilon_{\text{POC}})) - \varepsilon_{\text{POC}}) \cdot \ln(13.5 \text{ h} \cdot \beta + 1) + 13.5 \text{ h} \cdot \varepsilon_{\text{POC}} \cdot \beta}{\beta^2} \\ & - \frac{(\beta \cdot (1 + 9.5 \text{ h} \cdot (\delta_{\text{POC}} - \varepsilon_{\text{POC}})) - \varepsilon_{\text{POC}}) \cdot \ln(9.5 \text{ h} \cdot \beta + 1) + 9.5 \text{ h} \cdot \varepsilon_{\text{POC}} \cdot \beta}{\beta^2} \\ & + \frac{(\gamma \cdot (1 + 9.5 \text{ h} \cdot (\delta_{\text{POC}} - \varepsilon_{\text{POC}})) - \varepsilon_{\text{POC}} \cdot (1 + 13.5 \text{ h} \cdot (\beta - \gamma))) \cdot \ln(24 \text{ h} \cdot \gamma + 1 + 13.5 \text{ h} \cdot (\beta - \gamma)) + 24 \text{ h} \cdot \varepsilon_{\text{POC}} \cdot \gamma}{\gamma^2} \\ & - \frac{(\gamma \cdot (1 + 9.5 \text{ h} \cdot (\delta_{\text{POC}} - \varepsilon_{\text{POC}})) - \varepsilon_{\text{POC}} \cdot (1 + 13.5 \text{ h} \cdot (\beta - \gamma))) \cdot \ln(13.5 \text{ h} \cdot \gamma + 1 + 13.5 \text{ h} \cdot (\beta - \gamma)) + 13.5 \text{ h} \cdot \varepsilon_{\text{POC}} \cdot \gamma}{\gamma^2} \end{aligned} \right) \quad (3.1)$$

For $\gamma = 0$:

$$\text{POC quota}_{\text{mean}} = \frac{\text{POC quota}_{t_{\text{oh}}}}{24 \text{ h}} \cdot \left(\int_{0\text{h}}^{9.5\text{h}} \frac{1 + \delta_{\text{POC}} \cdot t}{1 + \beta \cdot t} dt + \int_{9.5\text{h}}^{13.5\text{h}} \frac{1 + \delta_{\text{POC}} \cdot 9.5 \text{ h} + \varepsilon_{\text{POC}} \cdot (t - 9.5 \text{ h})}{1 + \beta \cdot t} dt + \int_{13.5\text{h}}^{24\text{h}} \frac{1 + \delta_{\text{POC}} \cdot 9.5 \text{ h} + \varepsilon_{\text{POC}} \cdot (t - 9.5 \text{ h})}{1 + \beta \cdot 13.5 \text{ h}} dt \right)$$

$$= \frac{\text{POC quota}_{t_{\text{oh}}}}{24 \text{ h}} \cdot \left(\begin{aligned} & \frac{(\beta - \delta_{\text{POC}}) \cdot \ln(9.5 \text{ h} \cdot \beta + 1) + \delta_{\text{POC}} \cdot 9.5 \text{ h} \cdot \beta}{\beta^2} \\ & + \frac{(\beta \cdot (1 + 9.5 \text{ h} \cdot (\delta_{\text{POC}} - \varepsilon_{\text{POC}})) - \varepsilon_{\text{POC}}) \cdot \ln(13.5 \text{ h} \cdot \beta + 1) + 13.5 \text{ h} \cdot \varepsilon_{\text{POC}} \cdot \beta}{\beta^2} \\ & - \frac{(\beta \cdot (1 + 9.5 \text{ h} \cdot (\delta_{\text{POC}} - \varepsilon_{\text{POC}})) - \varepsilon_{\text{POC}}) \cdot \ln(9.5 \text{ h} \cdot \beta + 1) + 9.5 \text{ h} \cdot \varepsilon_{\text{POC}} \cdot \beta}{\beta^2} \\ & + \frac{1 + 9.5 \text{ h} \cdot (\delta_{\text{POC}} - \varepsilon_{\text{POC}})}{1 + 13.5 \text{ h} \cdot \beta} (24 \text{ h} - 13.5 \text{ h}) \\ & + \frac{\varepsilon_{\text{POC}}}{1 + 13.5 \text{ h} \cdot \beta} \cdot (24^2 \text{ h} - 13.5^2 \text{ h}) / 2 \end{aligned} \right) \quad (3.2)$$

Daily means are derived by taking the sum of the definite integrals of the functions expressing time-dependent cellular POC quotas in the different time intervals (Box 1) and dividing it by the length of all intervals (24 h). $\text{POC quota}_{t_{\text{oh}}}$ is the cellular POC quota (pg cell⁻¹) at the beginning of the dark phase t is the time of the day (h). δ_{POC} is the slope (h⁻¹) of the minor linear decrease in the relative POC concentrations before the start of the *production phase*. ε_{POC} is the slope (h⁻¹) of the linear increase in the relative POC concentration during the *production phase*. β is the slope (h⁻¹) of the increase in relative cell concentrations during the *division phase*, and γ is the slope of the minor decrease in relative cell concentrations after the end of the *division phase*. Equations 3.1 and 3.2 can similarly be applied to PIC quotas, replacing δ_{POC} with δ_{PIC} , and ε_{POC} with ε_{PIC} .

Box 4: Calculation of the daily mean of cellular production rates ($\text{pg cell}^{-1} \text{d}^{-1}$) of *E. huxleyi* cultures at the example of POC.:

For $\gamma \neq 0$:

$$\begin{aligned} \text{POC prod}_{\text{cell,mean}} &= \text{POC quota}_{t_{0h}} \cdot \left(\int_{0h}^{9.5h} \frac{\delta_{\text{POC}}}{1+\beta \cdot t} dt + \int_{9.5h}^{13.5h} \frac{\varepsilon_{\text{POC}}}{1+\beta \cdot t} dt + \int_{13.5h}^{24h} \frac{\varepsilon_{\text{POC}}}{1+\beta \cdot 13.5h + \gamma \cdot (t-13.5h)} dt \right) \\ &= \text{POC quota}_{t_{0h}} \cdot \left(\frac{\delta_{\text{POC}} \cdot \ln(9.5h \cdot \beta + 1)}{\beta} + \frac{\varepsilon_{\text{POC}} \cdot \ln(13.5h \cdot \beta + 1)}{\beta} - \frac{\varepsilon_{\text{POC}} \cdot \ln(9.5h \cdot \beta + 1)}{\beta} \right. \\ &\quad \left. + \frac{\varepsilon_{\text{POC}} \cdot \ln(24h \cdot \gamma + 1 + 13.5h \cdot (\beta - \gamma))}{\gamma} - \frac{\varepsilon_{\text{POC}} \cdot \ln(13.5h \cdot \gamma + 1 + 13.5h \cdot (\beta - \gamma))}{\gamma} \right) \end{aligned} \quad (4.1)$$

For $\gamma = 0$:

$$\begin{aligned} \text{POC prod}_{\text{cell,mean}} &= \text{POC quota}_{t_{0h}} \cdot \left(\int_{0h}^{9.5h} \frac{\delta_{\text{POC}}}{1+\beta \cdot t} dt + \int_{9.5h}^{13.5h} \frac{\varepsilon_{\text{POC}}}{1+\beta \cdot t} dt + \int_{13.5h}^{24h} \frac{\varepsilon_{\text{POC}}}{1+\beta \cdot 13.5h} dt \right) \\ &= \text{POC quota}_{t_{0h}} \cdot \left(\frac{\delta_{\text{POC}} \cdot \ln(9.5h \cdot \beta + 1)}{\beta} + \frac{\varepsilon_{\text{POC}} \cdot \ln(13.5h \cdot \beta + 1)}{\beta} - \frac{\varepsilon_{\text{POC}} \cdot \ln(9.5h \cdot \beta + 1)}{\beta} + \frac{\varepsilon_{\text{POC}} \cdot (24h - 13.5h)}{1+\beta \cdot 13.5h} \right) \end{aligned} \quad (4.2)$$

Daily means are derived by adding up the definite integrals of the functions expressing time-dependent cellular POC production rates in the different time intervals (cp. Eqs. 2.1, 2.3, 2.5 in Box 2). $\text{POC quota}_{t_{0h}}$ is the cellular POC quota (pg cell^{-1}) at the beginning of the dark phase. δ_{POC} is the slope (h^{-1}) of the minor linear decrease in the relative POC concentrations before the start of the *production phase*. ε_{POC} is the slope (h^{-1}) of the linear increase in the relative POC concentration during the *production phase*. β is the slope (h^{-1}) of the increase in relative cell concentrations during the *division phase*, and γ is the slope of the minor decrease in relative cell concentrations after the end of the *division phase*. Equations 4.1, 4.2 can similarly be applied to PIC quotas, replacing δ_{POC} with δ_{PIC} , and ε_{POC} with ε_{PIC} .

Box 5: Suggested simplifications of the presented models at the example of POC.:

Cell concentrations (cells mL⁻¹; modifications of Eqs. 10, 11):

$$N(t) = N_{t_{0h}} \cdot \left(1 + \frac{e^{\mu_{24h} \cdot 24h} - 1}{T_{DivP}} \cdot t \right) \quad \text{for } 0h \leq t \leq t_{End DivP} \quad (5.1)$$

$$N(t) = N_{t_{0h}} \cdot \left(1 + \frac{e^{\mu_{24h} \cdot 24h} - 1}{T_{DivP}} \cdot t_{End DivP} \right) \quad \text{for } t_{End DivP} \leq t \leq 24h \quad (5.2)$$

POC concentrations (pg mL⁻¹; modifications of Eqs. 13, 15):

$$POC(t) = POC_{t_{0h}} \quad \text{for } 0h \leq t \leq t_{Start ProdP} \quad (5.3)$$

$$POC(t) = POC_{t_{0h}} \cdot \left(1 + \frac{e^{\mu_{24h} \cdot 24h} - 1}{T_{ProdP}} \cdot (t - t_{Start ProdP}) \right) \quad \text{for } t_{Start ProdP} \leq t \leq 24h \quad (5.4)$$

Cellular POC quotas (pg cell⁻¹; modifications of Eqs. 1.1, 1.3, 1.5):

$$POC \text{ quota}(t) = POC \text{ quota}_{t_{0h}} \cdot \frac{1}{1 + \frac{e^{\mu_{24h} \cdot 24h} - 1}{T_{DivP}} \cdot t} \quad \text{for } 0h \leq t \leq t_{Start ProdP} \quad (5.5)$$

$$POC \text{ quota}(t) = POC \text{ quota}_{t_{0h}} \cdot \frac{1 + \frac{e^{\mu_{24h} \cdot 24h} - 1}{T_{ProdP}} \cdot (t - t_{Start ProdP})}{1 + \frac{e^{\mu_{24h} \cdot 24h} - 1}{T_{DivP}} \cdot t} \quad \text{for } t_{Start ProdP} \leq t \leq t_{End DivP} \quad (5.6)$$

$$POC \text{ quota}(t) = POC \text{ quota}_{t_{0h}} \cdot \frac{1 + \frac{e^{\mu_{24h} \cdot 24h} - 1}{T_{ProdP}} \cdot (t - t_{Start ProdP})}{1 + \frac{e^{\mu_{24h} \cdot 24h} - 1}{T_{DivP}} \cdot t_{End DivP}} \quad \text{for } t_{End DivP} \leq t \leq 24h \quad (5.7)$$

Cellular POC production rates (pg cell⁻¹ h⁻¹; modifications of Eqs. 2.1, 2.3, 2.5):

$$POC \text{ prod}_{cell}(t) = 0 \quad \text{for } 0h \leq t \leq t_{Start ProdP} \quad (5.8)$$

$$POC \text{ prod}_{cell}(t) = POC \text{ quota}_{t_{0h}} \cdot \frac{\frac{e^{\mu_{24h} \cdot 24h} - 1}{T_{ProdP}}}{1 + \frac{e^{\mu_{24h} \cdot 24h} - 1}{T_{DivP}} \cdot t} \quad \text{for } t_{Start ProdP} \leq t \leq t_{End DivP} \quad (5.9)$$

$$POC \text{ prod}_{cell}(t) = POC \text{ quota}_{t_{0h}} \cdot \frac{\frac{e^{\mu_{24h} \cdot 24h} - 1}{T_{ProdP}}}{1 + \frac{e^{\mu_{24h} \cdot 24h} - 1}{T_{DivP}} \cdot t_{End DivP}} \quad \text{for } t_{End DivP} \leq t \leq 24h \quad (5.10)$$

Mean POC quota (pg cell⁻¹; modification of Eq. 3.2):

$$\begin{aligned} POC \text{ quota}_{mean} = & POC \text{ quota}_{t_{0h}} \cdot \frac{\mu_{24h} \cdot T_{DivP}}{e^{\mu_{24h} \cdot 24h} - 1} \\ & \cdot \left\{ 1 + \frac{T_{DivP}}{T_{ProdP}} \cdot \left[\left(t_{Start ProdP} \cdot \frac{e^{\mu_{24h} \cdot 24h} - 1}{T_{DivP}} + 1 \right) \cdot \left(\frac{\ln \left(t_{Start ProdP} \cdot \frac{e^{\mu_{24h} \cdot 24h} - 1}{T_{DivP}} + 1 \right)}{\mu_{24h} \cdot 24h} - 1 \right) + \left(\frac{t_{End DivP} - t_{Start ProdP}}{24h} \right) \cdot \left(\frac{e^{\mu_{24h} \cdot 24h} - 1}{\mu_{24h} \cdot T_{DivP}} \right) \right] \right\} \\ & + POC \text{ quota}_{t_{0h}} \cdot \left[\left(e^{-\mu_{24h} \cdot 24h} - t_{Start ProdP} \frac{1 - e^{-\mu_{24h} \cdot 24h}}{T_{ProdP}} \right) \cdot \left(\frac{24h - t_{End DivP}}{24h} \right) + \left(\frac{1 - e^{-\mu_{24h} \cdot 24h}}{T_{ProdP}} \right) \cdot \left(\frac{24^2 h - t_{End DivP}^2 h}{2 \cdot 24h} \right) \right] \end{aligned} \quad (5.11)$$

Mean POC production rate (pg cell⁻¹ d⁻¹; modification of Eq. 4.2):

$$POC \text{ prod}_{cell, mean} = POC \text{ quota}_{t_{0h}} \cdot \left(\frac{T_{DivP}}{T_{ProdP}} \cdot \mu_{24h} \cdot 24h - \frac{T_{DivP}}{T_{ProdP}} \cdot \ln \left(t_{Start ProdP} \cdot \frac{e^{\mu_{24h} \cdot 24h} - 1}{T_{DivP}} + 1 \right) + \frac{e^{\mu_{24h} \cdot 24h} - 1}{e^{\mu_{24h} \cdot 24h}} \cdot (24h - t_{End DivP}) \right) \quad (5.12)$$

Continued

Box 5 Suggested simplifications of the presented models at the example of POC.—cont'd

Simplifications are: $\beta = \frac{M_{24h}}{T_{DivP}} = \frac{e^{\mu_{24h} \cdot 24h} - 1}{T_{DivP}}$, with β being the slope (h^{-1}) of the increase in relative cell concentrations during the *division phase*; $\gamma = 0 h^{-1}$, with γ being the slope of the decrease in relative cell concentrations after the end of the *division phase*; $\delta_{POC} = 0 h^{-1}$, with δ_{POC} being the slope of the linear decrease in the relative POC concentrations before the start of the *production phase*; and $\varepsilon_{POC} = \frac{M_{24h}}{T_{ProdP}} = \frac{e^{\mu_{24h} \cdot 24h} - 1}{T_{ProdP}}$, with ε_{POC} being the slope (h^{-1}) of the linear increase in the relative POC concentration during the *production phase*. T_{DivP} and T_{ProdP} are the length (h) of the *division* and *production phase*, respectively. $POC_{t_{0h}}$, $N_{t_{0h}}$, and $POC_{quota_{t_{0h}}}$ are the POC concentration ($pg mL^{-1}$), cell concentration ($cells mL^{-1}$), and the cellular POC quota ($pg cell^{-1}$) at the beginning of the dark phase. $t_{End DivP}$ is the time at which the *division phase* ends ($t_{End DivP} = T_{DivP}$; h) and $t_{Start ProdP}$ (h) is the time at which the *production phase* starts. Simplifications can only be made when cell mortality/degradation rates (cp. Eq. 11) and respiration rates (cp. Eq. 13) are small in relative terms.